

Factors Impeding Replacement of Ion Exchange with (Electro)Catalytic Treatment for Nitrate Removal from Drinking Water

Charles J. Werth,* Chenxu Yan, and Jacob P. Troutman



Cite This: <https://dx.doi.org/10.1021/acsestengg.0c00076>



Read Online

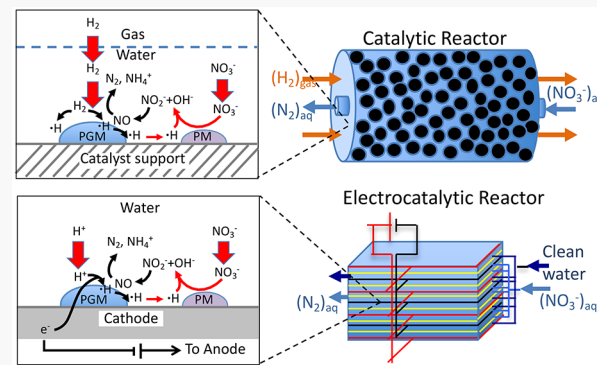
ACCESS |

Metrics & More

Article Recommendations

ABSTRACT: Nitrate (NO_3^-) has impacted more groundwater supplies than any other pollutant in the world. It is currently removed at water treatment plants by ion exchange, which is effective but comes at a steep financial and environmental cost. (Electro)catalytic treatment of nitrate has emerged as a promising alternative technology, which relies on reducing nitrate to dinitrogen gas or ammonium via reduction on a bimetal catalyst with atomic hydrogen oxidation. The bimetal catalyst contains a platinum group metal, and atomic hydrogen is either generated from supplied hydrogen gas (catalytic) or an applied current (electrocatalytic). However, (electro)catalytic treatment of nitrate is not being implemented at water treatment plants. This perspective addresses the most important technical challenges limiting widespread adoption of (electro)catalytic nitrate removal in drinking water treatment. These challenges affect precious metal amounts and cost, the efficiency and safety of hydrogen use, and end-product selectivity. This perspective is concluded by a prioritization of technology challenges, and their implications for attracting industry investment and achieving regulatory acceptance.

KEYWORDS: catalysis, electrochemical, nitrate, reduction



INTRODUCTION

Nitrate (NO_3^-) is the most common groundwater pollutant on the planet¹ and a seasonal surface water pollutant in active agriculture regions.² Nitrate primarily originates from nitrogen sources used in fertilizers for crops, where it drains from fields into groundwater and surface water.^{2,3} It also comes from animal feed lot runoff² and land application of municipal sludge for nutrients.^{4,5} Nitrate is problematic because it causes methemoglobinemia in those with weakened immune systems⁶ and because it transforms to carcinogenic nitrite (NO_2^-) and N-nitrosamines in the human body.⁷ The state-of-practice for NO_3^- removal from drinking water is ion exchange (IX). It is effective, reliable, and trusted, removing NO_3^- from treated drinking water to below regulatory levels for almost any finished drinking water quality. However, IX does not destroy nitrate but simply transfers it from one phase to another. Concentrated salt is then used to drive NO_3^- from exhausted IX resins, which is then discharged to the environment. The salt represents a considerable cost and can approach 80% of IX operations and maintenance costs.^{8,9} The salt discharged with concentrated nitrate in the waste brine also represents a significant environmental burden,^{10–14} contributing to salinization of local water resources¹⁵ and eutrophication.^{13,14}

Biological treatment has been eyed as a possible replacement to IX,¹⁶ and results in NO_3^- destruction to either innocuous dinitrogen (N_2) or ammonium (NH_4^+).^{17–20} The former end-product is preferred in water treatment, although efforts to create and economically concentrate the latter for a fertilizer source have been proposed. Unfortunately, biological treatment requires an added electron donor (often an organic chemical) and additional nutrients,^{18,20} which create conditions favorable for pathogen growth.¹⁶ Hence, downstream filtration and additional disinfection are needed;^{16,18,20} these increase costs and promote disinfection byproduct formation.²¹ Another challenge is biological reactor stability. Growing and maintaining a healthy NO_3^- reducing culture requires balancing nutrient requirements and maintaining relatively uniform water quality.^{17,18} This can be difficult for seasonally impacted surface water or for fluctuating water

Received: July 10, 2020

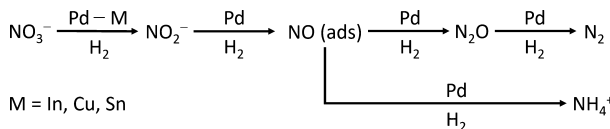
Revised: August 28, 2020

Accepted: August 31, 2020

quality or water quantity conditions. Another alternative is reverse osmosis. However, this approach is energy intensive and only considered when concurrent salt removal is desired.¹⁶ Like IX, reverse osmosis does not destroy NO_3^- but simply transfers it to a concentrated waste stream that requires disposal or further treatment.

Catalytic^{22–25} or electrocatalytic^{26,27} treatment addresses many of aforementioned concerns and limitations, and promotes rapid and on-demand NO_3^- destruction. The generally accepted reaction pathway for catalytic nitrate reduction is shown in **Scheme 1** and builds on the first report

Scheme 1. Proposed Reaction Pathways for Catalytic Nitrate Reduction



of this technology in 1989.²⁸ Atomic hydrogen ($\text{H}\cdot$) is created on a platinum group metal (PGM) surface from molecular hydrogen dissociation²⁵ or, in the case of electrocatalytic treatment, by combining an electron from an applied current with a proton in solution.²⁷ In the first step, the atomic hydrogen spills over from the PGM to a promoter metal (PM) for NO_3^- reduction to NO_2^- . Subsequent steps all occur on the PGM by direct reduction with atomic hydrogen.²⁹ The end products are N_2 and NH_4^+ ,^{25,30} and some control is possible with either material choice^{30,31} or reactor operating conditions.^{11,32,33}

The obvious advantages of (electro)catalytic treatment raise the obvious question of why the drinking water industry has not adopted this technology in place of IX for nitrate treatment. The primary reasons are cost and uncertainties in catalyst performance. Platinum group metals are expensive, and the amounts required depend on NO_3^- reduction activity and durability during water treatment.^{10,11,32–34} These factors vary from one study to the next, depending on reactor design,^{10,11,32–34} catalyst materials,^{25,31} and operating conditions.^{10,11,32–34} Also, hydrogen required for NO_3^- reduction can be expensive and potentially dangerous to transport and store. Many reactor designs in the literature inefficiently use this resource^{10,11,32–34} or require bulk hydrogen storage. These factors all hinder industry investment in technology transfer and the accompanying regulatory acceptance.

The objectives of this work are to provide a perspective on the most important technical challenges limiting widespread adoption of catalytic nitrate removal in drinking water treatment. These challenges affect precious metal amounts and cost, the efficiency and safety of hydrogen use, and end-product selectivity. These factors together all affect the willingness of industry to invest in catalytic treatment and work with regulators for approval. In this perspective, the costs of IX are compared to the costs of (electro)catalytic treatment, and the main drivers of costs for the latter are identified. Next, the rate-limiting reaction mechanisms affecting PGM use in water treatment are evaluated, followed by efforts to address these via improved reactor design and new material synthesis. Challenges for catalyst longevity are addressed next, followed by those for efficient and safe use of hydrogen, including end-product selectivity. This perspective is concluded by a prioritization of technology challenges, and their implications

for attracting industry investment and achieving regulatory acceptance.

COSTS FOR ION EXCHANGE AND (ELECTRO)CATALYTIC TREATMENT

An incomplete list of IX treatment systems used in the United States is presented in **Table 1**. Of the 25 listed, 19 continuously

Table 1. Examples of Ion Exchange (IX) Treatment Systems for Nitrate Removal Operating in the United States

utility	year starting operation	capacity (MGD)	ref
Glendale, AZ	2010	10	35, 36
Chino, CA	2006	7.2	37
Corona, CA	2018	3.5	38
Grover City, CA, 3 wells		2.3	39
La Crescenta, CA	1987	2.7	39
McFarland, CA, well 2	1983	1	39
McFarland, CA, well 4	1987	1	39
Porterville, CA	2006–2016	0.26 ^a	40
Indian Hills, CO	2009	0.07	37
Des Moines, IA	1992	10 (expanding to 20)	41, 42
Epworth, IA	2011	0.9	43, 44
Manchester, IA	2011	0.92	43, 44
Vale, ID	2006–2010	0.78	9
Bloomington, IL	2005	12.1	43
Columbus, IL	2017	80 ^b	45
Decatur, IL	2002	20	43
Streator, IL	2002	1.6	43, 44
Vermilion County, IL	2001	8	43
Adrian, MN	1998	0.13	46
Clear Lake, MN	1995	0.05	46
Edgerton, MN	2002	0.14	46
Ellsworth, MN	1994	0.05	46
Hastings, MN	2007	4.7	43
Bayard, NE	2018		47
McCook, NE	2006	7	9, 37

^aBased on personal communication with California Water Service Company. ^bTreatment plant is 80 MGD, but it is not clear if IX is treating the entire amount.

treat impacted groundwater and 6 seasonally treat impacted surface water. Seven of those listed have been in operation for over 20 years, and 20 for at least 10 years. The IX treatment systems serve mostly small communities, with 14 treating less than 3 million gallons per day (MGD). Only three of the systems treat more than 10 MGD. The limited sampling suggests that small communities located near current or former agricultural lands are impacted the most by nitrate contamination.

Costs for IX and (electro)catalytic treatment are presented in **Table 2**. They are expressed per 1000 gallons of water treated and assuming the NO_3^- concentration is equal to or twice the US Environmental Protection Agency's (U.S. EPA's) maximum contaminant level (MCL) of $44 \text{ mg } \text{NO}_3^- \text{ L}^{-1}$. For IX, the capital costs are amortized over a 20-year period. The cost for salt varies widely depending on location. Its percent of operations and maintenance (O&M) costs was reported in one study as 77%,⁹ and it is considered to be a dominant cost of treatment. Brine disposal costs can also be large, depending on the method employed, and can in some cases dominate.¹² The

Table 2. Cost of Ion Exchange (IX) and (Electro)Catalytic Treatment per 1000 Gallons of Water Treated

Ion Exchange (IX) ^a				
IX salt O&M ^b	IX disposal O&M ^c	IX total O&M ^d	IX capital ^d	IX total ^d
\$0.33, \$0.59	\$0.02–0.36	\$0.16–2.88 (\$0.95)	\$0.09–0.27 (\$0.16)	\$0.37–2.99 (\$1.15)
		\$0.21–7.92 (\$1.66)	NA	\$0.42–8.03 (\$1.86)
(Electro)Catalytic Treatment ^e				
H ₂ gas ^f	electricity for hydrogen ^g	Pd ^h	catalyst total ^h	electrocatalytic total ^h
\$0.05– 0.12	\$0.04	\$0.08	\$0.13–0.20	\$0.12
		\$0.31	\$0.36–0.43	\$0.35
		\$1.53	\$1.58–1.65	\$1.57

^aAll IX costs are in 2018 dollars. ^bFrom ref 9. The lower cost is for Vale, OR. The higher cost is for Fruitland, ID. ^cFrom ref 12. Values represent a range of costs for discharge to sanitary sewer, on-site evaporation in ponds and deep well injection. ^dFrom ref 37; based on USEPA cost estimating procedures for 0.17 to 1.09 MGD water treatment plant. Total O&M costs include salt and disposal. The lower range of costs is for treating 1 × MCL of nitrate, and the upper range of costs is for treating 2 × MCL of nitrate. Capital costs were only reported for treating 1 × MCL of nitrate. ^eAll (electro)catalytic costs are in 2018 dollars, except for Pd. The Pd cost is highly variable and is based on the 6/26/2020 spot price from <https://www.apmex.com/palladium-price>. Only hydrogen and Pd are considered in the totals. All other costs are ignored. ^fFrom ref 50; represents a range of prices from steam methane reforming (least expensive), to reformer-electrolyzer-purifier technology, to proton exchange membrane (most expensive). ^gBased on direct H₂ production in an electrocatalytic cell with 50% current efficiency and average cost (6 cents per kWh) of electricity for industry from Austin, TX, in 2018.⁵¹ ^hValues reflect Pd replacement times of 20, 5, and 1 year, respectively. Pd costs are based on nitrate reduction activities in a trickle-bed reactor from ref 34.

least expensive options considered are discharge to the sanitary sewer and on-site evaporation ponds, and the most expensive is deep well injection.

Only hydrogen and palladium (Pd) costs are considered for (electro)catalytic treatment, as these are expected to dominate.^{11,48} Promoter metal costs are neglected because (as described below), they typically comprise <20 wt % of PGMs in NO₃[–] reduction catalysts and are relatively inexpensive on an equivalent mass basis (e.g., <1% of PGM costs, APMEX, Inc. and RotoMetals; as of 6/29/2020). Treatment from 88 (2 × MCL) to 22 mg NO₃[–] L^{–1} is assumed. For catalytic treatment, hydrogen gas costs were

determined from the literature assuming either steam methane reforming (least expensive) or electrochemical generation. For electrocatalytic treatment, electricity costs required to generate hydrogen *in situ* were determined from our recent work assuming ~50% hydrogen use efficiency for NO₃[–] reduction to N₂.⁴⁹ Pd costs were determined assuming reaction kinetics from a trickle bed reactor, and either a 20-, 5-, or 1-year Pd life span. Faster kinetics have been realized for electrocatalytic reactors, and these will be discussed in a subsequent section. Based on catalytic systems used in the petrochemical industry, a 20-year life span is likely not realistic. However, Pd is typically recovered from deactivated catalysts and reused, and this is not considered due to the lack of sufficient economic data.

The costs for hydrogen are always lower for electrocatalytic reduction. The costs for Pd vary from \$0.08, \$0.31, to \$1.53, depending on whether the Pd is replaced after 20, 5, or 1 years. The Pd costs dominate total costs for the 5- and 1-year life spans. In comparison to IX, costs for (electro)catalytic treatment are generally comparable or lower, primarily depending on catalyst life. This suggests that costs for (electro)catalytic treatment of NO₃[–] are competitive with IX but do not yet offer a clear advantage. The primary barrier is the cost for Pd. An (electro)catalytic reactor with 10 times the activity of the trickle bed reactor would decrease these costs by the same factor and could completely reverse the economics. In contrast, a Pd catalyst requiring replacement every three months due to irreversible fouling would likely be prohibitively expensive. The costs also make clear that hydrogen must be used efficiently. A 10% efficiency of hydrogen use would balloon costs and make the system noncompetitive. Hence, lower Pd use and efficient hydrogen use are necessary to advance the technology.

RATE LIMITING NITRATE REDUCTION MECHANISMS DRIVING PLATINUM GROUP METAL USE

Potential rate limiting steps for (electro)catalytic nitrate reduction identified through batch and flow-through reactor, and molecular modeling studies are highlighted in Figure 1. In catalytic systems, NO₃[–] adsorbs to reduced or partially reduced sites on the PM surface, which are thought to oxidize and reduce NO₃[–] to NO₂[–]. These sites are then rereduced by reaction with spilled over atomic hydrogen from the PGM.^{52–54} In electrocatalytic systems, NO₃[–] also adsorbs to the PM surface for reduction to NO₂[–], but there is no data indicating whether the surface oxidation state changes or if

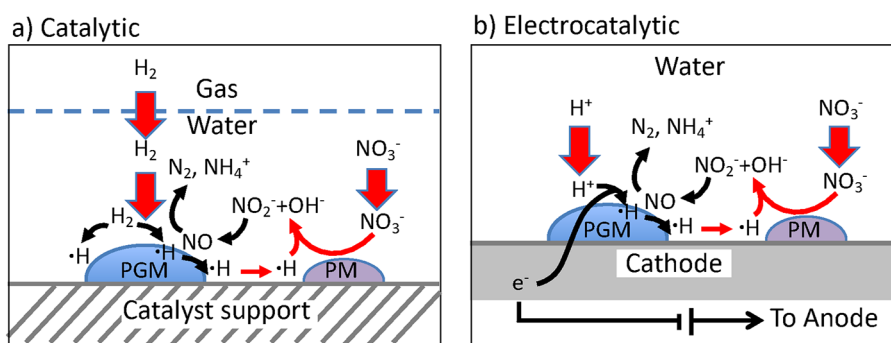


Figure 1. Reaction pathways (all arrows) and potential rate limiting steps (red arrows) for nitrate reduction in (a) catalytic versus (b) electrocatalytic reactors. PGM refers to platinum group metal, and PM refers to promoter metal.

atomic hydrogen directly reacts with NO_3^- . Formed NO_2^- migrates to the PGM for further reduction to dinitrogen or ammonium. This reaction can be limited by the rate of nitrate reduction at the PM surface, the rate of atomic hydrogen spillover from the PGM, or atomic hydrogen generation.

Density functional theory (DFT) studies examining indium ensembles on a Pd(111) surface revealed that the rate of NO_3^- reduction depends primarily on PM ensemble shape. The configuration of indium atoms in these small ensembles impacts both the adsorption binding energy of NO_3^- and the activation barrier for the nitrate-to-nitrite reduction step. Indium 4-mers (four atom ensembles; corresponding to 25% surface coverage of a catalyst) result in substantial improvement for NO_3^- reduction as the ensemble is able to better stabilize NO_3^- , the intermediate $[\text{NO}_2-\text{O}]^*$, and the abstracted oxygen. These calculations match closely with experimental results for NO_3^- reduction on indium-decorated Pd catalysts.⁵⁴

The rate of atomic hydrogen spillover primarily depends on the distance between the PGM and the PM and on the material used to support the active metals. As expected, the closer the distance between the PGM and the PM, the faster spillover occurs. However, this spillover rate varies dramatically between materials. Reducible metal oxides (e.g., TiO_2 or CeO_2) transport atomic hydrogen as a proton–electron combination; the electron reduces the cation species of the oxide support (e.g., Ti(IV) to Ti(II) or Ce(IV) to Ce(III)), while the proton binds to surface oxygen anions, resulting in a net hydrogen migration.⁵⁵ On nonreducible supports (e.g., SiO_2 or Al_2O_3), hydrogen spillover is often accredited to surface contamination/defects. However, proof of spillover on these materials is rare, hard to confirm, and energetically unfavorable.^{55,56} First-principles atomistic simulations of hydrogen spillover on TiO_2 yield diffusion coefficients on the order of $10^{-14} \text{ cm}^2 \text{ s}^{-1}$; additionally, the mobility of the H^+/e^- pair is not hindered by the presence of water. Similar studies for Al_2O_3 supports yield diffusion coefficients on the order of $10^{-23}\text{--}10^{-25} \text{ cm}^2 \text{ s}^{-1}$, significantly slower than on TiO_2 .^{55,57}

Atomic hydrogen generation at the PGM surface proceeds through a series of steps, and some of these may be rate limiting. In catalytic systems, molecular hydrogen is supplied in the gas phase; its mass transfer to the water phase can limit reaction rates.³³ Furthermore, aqueous phase mass transfer of hydrogen or NO_3^- to the catalyst surface can limit overall NO_3^- reaction rates. This can occur in bulk solutions that are not well mixed, or within larger porous particles used to support active catalyst metals. The adsorption and dissociation of molecular hydrogen to atomic hydrogen occurs significantly faster than NO_2^- hydrogenation,^{52,53} as it faces little energetic barrier.^{58–60} In electrocatalytic systems, atomic hydrogen can be directly generated at the PGM surface by combining electrons from an applied current with protons in solution. Below the standard reduction potential of atomic hydrogen formation and above the standard reduction potential of molecular hydrogen formation, this step may be rate limiting due to the low supply of atomic hydrogen as the reductant.⁶¹ However, below the standard reduction potential of molecular hydrogen formation, copious gas evolution in batch and flow through reactors indicates this process is fast relative to other steps during NO_3^- reduction. Nonetheless, recombination of atomic hydrogen to H_2 gas consumes the atomic hydrogen and restrains the migration of electrons and ions on the catalyst surface, which can possibly inhibit the rate of reaction.^{61,62}

Nitrite formed at the PM site transfers to the PGM by surface diffusion, or by desorbing and readsorbing; it can then react with atomic hydrogen. In most batch studies at circumneutral pH, very little NO_2^- accumulates; this indicates that surface diffusion dominates NO_2^- transfer from the PM to the PGM, and NO_2^- reduction is not rate limiting.^{30,52,53,63} Spectroscopic evidence indicates that NO_2^- reacts to form adsorbed NO, which then reacts to form either nitrous oxide (N_2O) en route to N_2 or NH_4^+ .^{64,65} The intermediate NO has never been observed in solution.^{66,67} The intermediate N_2O has been observed in solution and in off gas, and complete mass balances of NO_3^- consumed versus N_2 or NH_4^+ produced indicates it reacts faster than NO_3^- or NO_2^- if maintained in a closed reactor.^{67–69} Hence, steps beyond NO_3^- reduction are usually not considered rate limiting under anticipated reaction conditions. Exceptions occurs at elevated pH (*i.e.*, $\text{pH} \geq 7$).⁷⁰ Both NO_3^- and NO_2^- reduction yield hydroxide (OH^-) as a reaction product. Under acidic conditions or in the presence of sufficient buffer, this product is neutralized. However, if pH values increase, the surface charge on (electro)catalysts becomes increasingly negative, which results in electrostatic repulsion of NO_3^- and NO_2^- ions.^{29,71} Additionally, pH influences the adsorbed surface species on the catalyst; at lower pH values, the catalyst surface is mostly covered with hydrogen species, while at higher pH values, the surface is covered with OH^- ions or even oxides. These species block the readsorption of NO_2^- to the PGM, resulting in a buildup of aqueous NO_2^- .²⁹ It is speculated that the deoxygenation of adsorbed NO_2^- is assisted by protons.^{23,72} Once adsorbed, NO_2^- is protonated at one oxygen and the N–O bond of the hydroxide is cleaved to yield adsorbed NO. Because of the need for protons, this process is significantly slowed by higher pH values.

Not illustrated in Figure 1 is electrochemical nitrate reduction by direct charge transfer.²⁷ The first step is considered rate limiting and involves nitrate adsorption on the cathode and a three-step electrochemical–chemical–electrochemical (ECE) mechanism to form nitrite. Next, a two-electron transfer to nitrite forms a dianion radical NO_2^{2-} , that quickly hydrolyzes to form $\text{NO}(\text{ads})$. Several different reaction pathways are then possible, yielding either N_2 or NH_4^+ . The relative contributions of hydrogenation versus direct charge transfer for nitrate reduction in electrocatalytic systems requires further elucidation, but generally there is more hydrogenation on cathodes containing PGMs.

■ EFFORTS TO REDUCE PLATINUM GROUP METAL USE THROUGH REACTOR DESIGN

Small batch reactors often used in the laboratory can be operated at high mixing and hydrogen delivery rates to eliminate external particle mass transfer and hydrogen limitations,^{73–76} yielding the fastest reduction rates possible for a given catalyst material. These are often called intrinsic reaction rates, even though intraparticle mass transfer may still be limiting.^{76–78} In contrast, large batch reactors capable of treating NO_3^- at a drinking water plant commonly suffer from mass transfer limitations due to stagnant zones and slow mixing. They also are expected to suffer from PGM losses as catalyst particles collide and break apart over extended treatment times, and from energy, maintenance, and material costs associated with emptying and filling batch reactors. Consequently, large-scale batch reactors are not considered practical for NO_3^- removal in water treatment plants, and flow-

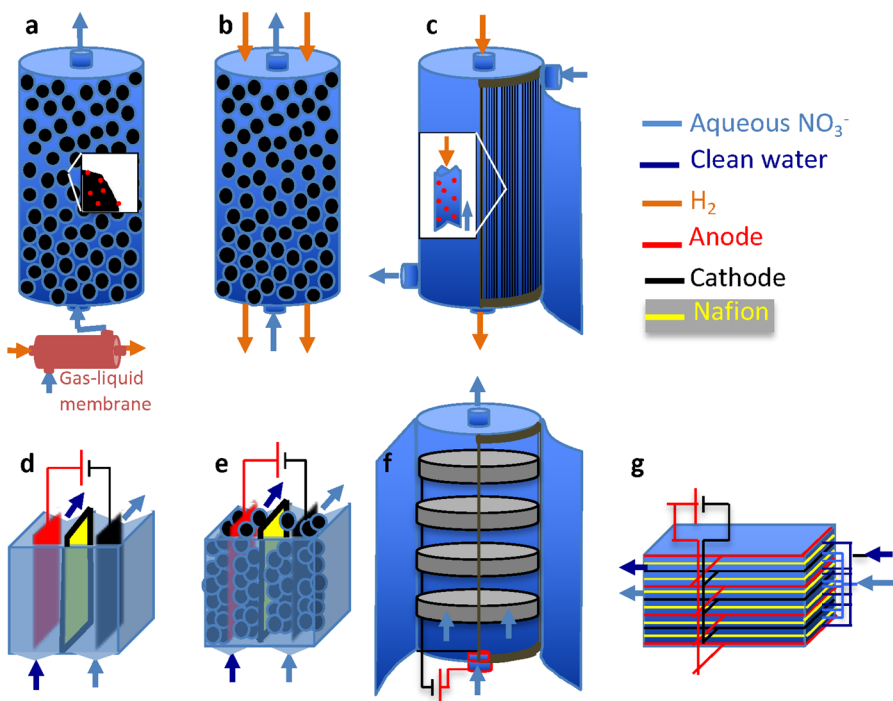


Figure 2. Illustration of (a–c) catalytic and (d–g) electrocatalytic reactor types: (a) Single-fluid packed bed reactor; (b) Dual-fluid packed bed reactor; (c) Membrane reactor; (d) Plate-in-tank reactor; (e) Fluidized or packed bed reactor with inert or catalytically active particles; (f) Membrane flow-through reactor; (g) Thin-layer reactor.

through reactors with fixed catalysts that take advantage of the available hydraulic head are preferred. Examples of these are presented in Figure 2.

Catalytic flow-through reactor designs include single-fluid packed bed,^{79–84} dual-fluid packed bed,^{10,11,32,34,85–88} and membrane reactors^{89–91} (Figure 2a–c), all with molecular hydrogen supplied as the electron donor. Overall reaction rate constant comparisons and reaction times for treating an 80 mg $\text{NO}_3^- \text{ L}^{-1}$ solution to 40 mg $\text{NO}_3^- \text{ L}^{-1}$ using 1 g PGM L^{-1} catalysts are provided in Table 3. Reaction times are easier to compare among different reactors with different reaction orders and rate constant normalizations. The NO_2^- and NO_3^- reaction times in batch reactors are the shortest, as low as 0.01 and 0.09 min, respectively. Only NO_3^- reaction times are listed for flow-through reactors, and the shortest is 2.1 min for a trickle-bed reactor.

With the single-fluid reactor type, hydrogen is dissolved in water using a gas–liquid membrane module,⁸³ or by presparging water before treatment,^{79–82,84} and the fluid flows through a fixed bed of mm-size supported catalysts. At ambient conditions, such reactors are limited to treating low (0.2–0.32 mM or 12.4–19.8 mg $\text{NO}_3^- \text{ L}^{-1}$) NO_3^- concentrations because of hydrogen solubility limits. For comparison, the maximum contaminant limit allowed in drinking water is approximately 44 mg $\text{NO}_3^- \text{ L}^{-1}$.³ At elevated pressure, more hydrogen can be dissolved into solution,⁷⁹ but with an anticipated steep trade-off in capital costs for high-pressure equipment.

With the dual-fluid reactor type, hydrogen is added in the gas phase counter or with the direction of water flow, also through a fixed bed of mm-size supported catalysts. This arrangement allows treatment of dilute to concentrated NO_3^- streams, but gas-to-water mass transfer for hydrogen limits overall treatment rates. The best rates obtained in the literature

for this design were from a trickle bed reactor operated in counter-current mode.^{33,34} Over the range of gas and liquid flow rate tested, the maximum overall rate constant was still at best 18% of the rate constant obtained for the same catalyst in a small batch reactor.³⁴

Membrane-based reactors are a relatively new approach, with supported catalysts embedded on the water-side of flat-sheet or hollow-fiber polymeric membranes.^{89–91} Molecular hydrogen flows through the gas-side of the membranes and diffuses across to the water side to reduce nitrate at catalyst sites. Few peer-reviewed publications present this approach. In one study,⁹¹ Pd and Cu supported on Al_2O_3 particles were deposited on both flat sheet and hollow fiber polyetherimide (PEI) ultrafiltration membranes. Nitrate reduction activity was demonstrated, but comparisons to batch studies and Pd loadings were not provided for easy comparison. In another study,⁸⁹ Pd with In, Cu, or Sn were loaded onto Al_2O_3 particles and deposited on hollow fiber tubes in a loop dialyzer. The best NO_3^- reduction activity was only ~17% of that in batch, indicating significant mass transfer limitations. The longest time period of continuous operation for these systems was 60 days, and no loss in membrane integrity or catalyst activity was reported. In the third study,⁹⁰ different reaction conditions were investigated in a flow-through hollow fiber membrane reactor with recirculation, the results of which were reported in percent removal. Room temperature, lower liquid flow rate, higher H_2 pressure and initial NO_2^- concentration all facilitated nitrite removal kinetics. It was also demonstrated that flow-through mode (H_2 -saturated medium diffusing through the catalytic hollow fiber membrane when flowing through the reactor) provided better removal efficiency over two-phase counter flow mode. However, the flow-through operation requires higher operating pressure, which can lead to higher energy consumption and cost.

Table 3. Summary of Published Rate Constants for (Electro)Catalytic Nitrate and Nitrite Reduction and Estimated Reaction Times to Reduce 80–40 mg L⁻¹ of either Nitrate or Nitrite

reaction type	electrode or catalyst material ^a	compound of interest	reactor configuration	reaction conditions	activity	time (min) ^e	ref
electrocatalytic	0.86 wt % Pd 0.07 wt % In/ACF	nitrite	PPTL reactor, recirculation mode	-0.778 V vs SHE -0.378 V vs SHE	$14.3 \times 10^{-3} \text{ min}^{-1}$ or $0.57 \text{ L g}_{\text{Pd}}^{-1} \text{ min}^{-1}$	1.2	49
	0.86 wt % Pd 0.07 wt % In/ACF	nitrite	PPTL reactor, recirculation mode		$9.5 \times 10^{-3} \text{ min}^{-1}$ or $0.38 \text{ L g}_{\text{Pd}}^{-1} \text{ min}^{-1}$	1.8	49
Pt	Cu ₁₇ Pt ₈₃	nitrite	membrane/electrode assembly (MEA), batch mode	100 mA	$1.6 \times 10^{-3} \text{ min}^{-1c}$	433.2	108
	Rh–Pt ^b	nitrite	membrane/electrode assembly (MEA), batch mode	100 mA	$4.2 \times 10^{-3} \text{ min}^{-1c}$	165.0	108
	Ag ₁₄ Pt ₈₆	nitrite	membrane/electrode assembly (MEA), batch mode	100 mA	$23.1 \times 10^{-3} \text{ min}^{-1c}$	30.0	108
	Ni ₉ Pt ₉₁	nitrite	membrane/electrode assembly (MEA), batch mode	100 mA	$4.1 \times 10^{-3} \text{ min}^{-1c}$	169.1	108
	Pd	nitrite	membrane/electrode assembly (MEA), batch mode	100 mA	$12.3 \times 10^{-3} \text{ min}^{-1c}$	56.4	108
	Cu ₃₈ Pd ₆₂	nitrite	membrane/electrode assembly (MEA), batch mode	100 mA	$2.9 \times 10^{-3} \text{ min}^{-1c}$	239.0	102
	Pt ₅₅ Pd ₄₅	nitrite	membrane/electrode assembly (MEA), batch mode	100 mA	$13.9 \times 10^{-3} \text{ min}^{-1c}$	49.9	102
	Ni ₆ Pd ₉₄	nitrite	membrane/electrode assembly (MEA), batch mode	100 mA	$1.6 \times 10^{-3} \text{ min}^{-1c}$	433.2	109
	Ag ₃₀ Pd ₇₀	nitrite	membrane/electrode assembly (MEA), batch mode	100 mA	$8.1 \times 10^{-3} \text{ min}^{-1c}$	85.57	109
	8 wt % Rh 92 wt % Pd	nitrite	membrane/electrode assembly (MEA), batch mode	100 mA	$4.1 \times 10^{-3} \text{ min}^{-1c}$	169.1	109
	8 wt % Rh 92 wt % Pd	nitrite	membrane/electrode assembly (MEA), batch mode	100 mA	$25.6 \times 10^{-3} \text{ min}^{-1c}$	27.1	109
	Rh/graphite	nitrite	two-compartment electrochemical cell separated by a Nafion 117 membrane, batch mode	-1.001 V vs SHE 4 mA/cm ²	$45.0 \times 10^{-3} \text{ min}^{-1c}$	15.4	109
					$1.2 \times 10^{-3} \text{ min}^{-1c}$	577.6	110
	2 wt % Pd 1 wt % In/Ti _n O _{2n-1}	nitrate	flow-through membrane reactor, continuous flow mode	-2.5 V vs SHE	$1.6 \times 10^{-2} \text{ L g}_{\text{Pd}}^{-1} \text{ min}^{-1}$	43.3	26
	2 wt % Pd 1 wt % Cu/Ti _n O _{2n-1}	nitrate	flow-through membrane reactor, continuous flow mode	-2.5 V vs SHE	$2.4 \times 10^{-2} \text{ L g}_{\text{Pd}}^{-1} \text{ min}^{-1}$	28.9	26
	Cu ₁₅ Pt ₈₅	nitrate	membrane/electrode assembly (MEA), continuous flow mode	100 mA	$4.1 \times 10^{-3} \text{ min}^{-1c,d}$	169.1	102
	Cu ₃₃ Pd ₆₇	nitrate	membrane/electrode assembly (MEA), continuous flow mode	100 mA	$17.4 \times 10^{-3} \text{ min}^{-1c,d}$	39.8	102
	Cu ₁₅ Pt ₈₅	nitrate	membrane/electrode assembly (MEA), batch mode	100 mA	$17.8 \times 10^{-3} \text{ min}^{-1c}$	38.9	102
	Cu ₃₈ Pd ₆₂	nitrate	membrane/electrode assembly (MEA), batch mode	100 mA	$49.0 \times 10^{-3} \text{ min}^{-1c}$	14.2	102
	Pt ₅₅ Pd ₄₅	nitrate	membrane/electrode assembly (MEA), batch mode	100 mA	$14.0 \times 10^{-3} \text{ min}^{-1c}$	49.5	109
	Ag ₃₀ Pd ₇₀	nitrate	membrane/electrode assembly (MEA), batch mode	100 mA	$50.7 \times 10^{-3} \text{ min}^{-1c}$	13.7	109
	8 wt % Rh 92 wt % Pd	nitrate	membrane/electrode assembly (MEA), batch mode	100 mA	$21.1 \times 10^{-3} \text{ min}^{-1c}$	33.0	109
	Cu	nitrate	parallel-plate, undivided cell, recirculation mode	3.8 mA cm ⁻²	$4.3 \times 10^{-3} \text{ min}^{-1c,d}$	161.2	93
	Sn	nitrate	two-compartment electrochemical cell separated by a Nafion 117 membrane, batch mode	-2.9 V vs Ag/AgCl ^f	$1.0 \times 10^{-1} \text{ min}^{-1c}$	6.7	111
			plate-in-tank reactor	40 mA	$6.9 \text{ mg NO}_3^- \text{ min}^{-1} \text{ g}_{\text{Pd}}^{-1}$	5.8	112
			conventional three-electrode batch cell	-0.79 V vs SHE	$13.4 \times 10^{-3} \text{ min}^{-1c}$	51.8	113
			single compartment batch cell	-1.006 V vs SHE	27.6 min ⁻¹	0.03	94
			packed bed reactor	600 V	$1.0 \times 10^{-1} \text{ min}^{-1}$	6.7	99
			fluidized bed reactor with catalytically active particles	30 mA	$19.0 \times 10^{-3} \text{ min}^{-1}$	36.5	114
			batch	H ₂ ; 135 mL min ⁻¹	$10.1 \text{ L g}_{\text{Pd}}^{-1} \text{ min}^{-1}$	0.07	22
	5 wt % Pd 1.25 wt % Sn/ACF	nitrate			$6.9 \text{ mg NO}_3^- \text{ min}^{-1} \text{ g}_{\text{Pd}}^{-1}$	5.8	
	Pd–Cu/graphite ^b	nitrate			$13.4 \times 10^{-3} \text{ min}^{-1c}$	51.8	
	Cu ₇₀ Ni ₃₀	nitrate			27.6 min ⁻¹	0.03	94
	Fe	nitrate			$1.0 \times 10^{-1} \text{ min}^{-1}$	6.7	99
	Pd–Sn/AC (4:1, w:w)	nitrate			$19.0 \times 10^{-3} \text{ min}^{-1}$	36.5	114
	5.0 wt % Pd 1.5 wt % Cu/γ-Al ₂ O ₃	nitrate			$10.1 \text{ L g}_{\text{Pd}}^{-1} \text{ min}^{-1}$	0.07	22
	Pd ₅₅ Au ₄₇ NPs/SiO ₂	nitrate	batch	H ₂ ; 120 mL min ⁻¹ , 1 h	$13.7 \text{ L g}_{\text{Pd}}^{-1} \text{ min}^{-1}$	0.05	24
	Pd ₉₅ Ag ₅ NPs/SiO ₂	nitrate	batch	H ₂ ; 120 mL min ⁻¹ , 1 h	$4.6 \text{ L g}_{\text{Pd}}^{-1} \text{ min}^{-1}$	0.15	115
	Pd ₈₀ Cu ₂₀ colloids	nitrate	batch	H ₂ ; 60 mL min ⁻¹ , 20 min	$1.9 \text{ L g}_{\text{Pd}}^{-1} \text{ min}^{-1}$	0.36	23

Table 3. continued

reaction type	electrode or catalyst material ^a	compound of interest	reactor configuration	reaction conditions	activity	time (min) ^c	ref
5.0 wt % Pd/CNF	nitrite	batch	H ₂ ; 135 mL min ⁻¹	36.6 L g _{Pd} ⁻¹ min ⁻¹	0.02	76	
5.0 wt % Pd/ γ -Al ₂ O ₃	nitrite	batch	H ₂ ; 135 mL min ⁻¹	4.4 L g _{Pd} ⁻¹ min ⁻¹	0.16	76	
1.0 wt % Pd/ γ -Al ₂ O ₃	nitrite	batch	P _{H₂} ; 0.32 bar	48.0 L g _{Pd} ⁻¹ min ⁻¹	0.01	75	
Pd/PVP	nitrite	hollow fiber membrane	H ₂ ; 0.85 mM	6.7 mg NO ₃ ⁻ min ⁻¹ g _{Pd} ⁻¹	6.0	89	
5.0 wt % Pd	nitrate	batch	H ₂ ; 135 mL min ⁻¹	4.7 L g _{Pd} ⁻¹ min ⁻¹	0.15	22	
1.5 wt % Cu/ γ -Al ₂ O ₃ Pd ₈₀ Cu ₂₀ colloids	nitrate	batch	H ₂ ; 60 mL min ⁻¹ , 20 min	0.12 L g _{Pd} ⁻¹ min ⁻¹	6.0	23	
5.0 wt % Pd 1.25 wt % Cu/AC	nitrate	batch	H ₂ ; 400 mL min ⁻¹	6.4 L g _{Pd} ⁻¹ min ⁻¹	0.11	116	
5.0 wt % Pd 1.0 wt % In/AC	nitrate	batch	H ₂ ; 400 mL min ⁻¹	7.6 L g _{Pd} ⁻¹ min ⁻¹	0.09	116	
5.0 wt % Pd 1.25 wt % Sn/AC	nitrate	batch	H ₂ ; 400 mL min ⁻¹	6.6 L g _{Pd} ⁻¹ min ⁻¹	0.11	116	
5.0 wt % Pd	nitrate	batch	P _{H₂} ; 0.46 bar	3.2 L g _{Pd} ⁻¹ min ⁻¹	0.21	73	
1.4 wt % Cu/ γ -Al ₂ O ₃	nitrate	batch	H ₂ ; 120 mL min ⁻¹ , 1 h	5.0 L g _{Pd} ⁻¹ min ⁻¹	0.14	117	
5.0 wt % Pd 1.5 wt % Cu/ZrO ₂	nitrate	batch	H ₂ ; 135 mL min ⁻¹	3.4 L g _{Pd} ⁻¹ min ⁻¹	0.20	118	
5.0 wt % Pd 1.0 wt % In/ γ -Al ₂ O ₃	nitrate	batch	P _{H₂} ; 1.0 bar	117 mg NO ₃ ⁻ min ⁻¹ g _{Pd} ⁻¹	0.3	70	
5 wt % Pd 0.83 wt % Sn/Al ₂ O ₃	nitrate	batch	H ₂ ; 120 mL min ⁻¹ , 1 h	333 mg NO ₃ ⁻ min ⁻¹ g _{Pd} ⁻¹	0.1	71	
4.9 wt % Pd 1.5 wt % Cu/ZrO ₂	nitrate	batch	H ₂ ; 0.8 mM	5.4 ± 0.3 mg NO ₃ ⁻ min ⁻¹ g _{Pd} ⁻¹	7.4	11	
2.5 wt % Pd 0.25 wt % In/C	nitrate	dual-fluid packed bed	H ₂ ; 0.8 mL min ⁻¹	2.24 ± 0.22 mg NO ₃ ⁻ min ⁻¹ g _{Pd} ⁻¹	17.9	10	
0.5 wt % Pd 0.05 wt % In/C	nitrate	dual-fluid packed bed	H ₂ ; 90 mL min ⁻¹	17.4 ± 0.04 mg NO ₃ ⁻ min ⁻¹ g _{Pd} ⁻¹	2.3	33	
0.5 wt % Pd 0.05 wt % In/AC	nitrate	trickle bed	H ₂ ; ~300 mL min ⁻¹	19.5 ± 1.3 mg NO ₃ ⁻ min ⁻¹ g _{Pd} ⁻¹	2.1	34	
0.1 wt % Pd 0.01 wt % In/ γ -Al ₂ O ₃	nitrate	trickle bed	P _{H₂} ; 0.3 bar	2.03 mg NO ₃ ⁻ min ⁻¹ g _{Pd} ⁻¹	20.0	32	
1.0 wt % Pd 0.3 wt % Cu/ γ -Al ₂ O ₃	nitrate	bubble column fixed bed	P _{H₂} ; 0.3 bar	1.31 mg NO ₃ ⁻ min ⁻¹ g _{Pd} ⁻¹	30.8	32	
1.0 wt % Pd 0.3 wt % Cu/ γ -Al ₂ O ₃	nitrate	trickle bed	H ₂ ; 50 mL min ⁻¹	6.1 mg NO ₃ ⁻ min ⁻¹ g _{Pd} ⁻¹	6.6	85	
0.25 wt % Pd 0.25 wt % Cu/AC	nitrate	trickle bed	H ₂ ; 0.85 mM	5.5 mg NO ₃ ⁻ min ⁻¹ g _{Pd} ⁻¹	7.3	70	
5 wt % Pd 1 wt % In/Al ₂ O ₃	nitrate	hollow fiber membrane reactor	H ₂ ; 0.85 mM	6.4 mg NO ₃ ⁻ min ⁻¹ g _{Pd} ⁻¹	6.2	89	
5 wt % Pd 1.25 wt % Sn/Al ₂ O ₃	nitrate	hollow fiber membrane reactor	P _{H₂} ; 2.0 bar	9.2 mg NO ₃ ⁻ min ⁻¹ g _{Pd} ⁻¹	4.4	77	
4.1 wt % Pd 1.0 wt % Sn/Al ₂ O ₃	nitrate	stirred-tank membrane reactor	P _{H₂} ; 2.09 atm	~0.53 mg NO ₃ ⁻ min ⁻¹ g _{Pd} ⁻¹	75.5	119	
1.6 wt % Pd 1.2 wt % Cu/ceramic	nitrate	membrane reactor	P _{H₂} ; 6.0 bar	17.6 mg NO ₃ ⁻ min ⁻¹ g _{Pd} ⁻¹	2.3	79	
1.0 wt % Pd 0.3 wt % Cu/ACC	nitrate	single-fluid packed bed	P _{H₂} ; 1.0 bar	6.2 mg NO ₃ ⁻ min ⁻¹ g _{Pd} ⁻¹	6.4	92	
Pd ₇₁ Cu ₂₉ /Al ₂ O ₃	nitrate	membrane reactor	H ₂ ; 6.0 mL min ⁻¹	7.6 mg NO ₃ ⁻ min ⁻¹ g _{Pd} ⁻¹	5.2	86	
1 wt % Pd 0.25 wt % In/Al ₂ O ₃	nitrate	dual-fluid packed bed	P _{H₂} ; 0.96 atm	6.2 mg NO ₃ ⁻ min ⁻¹ g _{Pd} ⁻¹	6.5	87	
1 wt % Pd	nitrate	dual-fluid packed bed	H ₂ ; 7.0 mL min ⁻¹	3.9 mg NO ₃ ⁻ min ⁻¹ g _{Pd} ⁻¹	10.2	80	
0.5 wt % Cu/TiO ₂ –Al ₂ O ₃	nitrate	dual-fluid packed bed					
3 wt % Pt 1.5 wt % Ag/AC	nitrate						

Table 3. continued

^aMaterial compositions are expressed in molar ratio unless otherwise stated. ^bMetal loadings or ratios are not presented in the references. ^cActivity with units of inverse minutes represent first-order rate constants that are not normalized to 1 g Pd L⁻¹ due to unavailability of mass of PGM in the references for electrocatalytic reduction. ^dValues are approximated from figures in the references. ^eReaction time assuming reduction of an 80 mg NO₃⁻ L⁻¹ to 40 mg NO₃⁻ L⁻¹ using 1 g PGM L⁻¹ catalysts. This allows comparison of reduction activity across different catalyst/cathode materials, types of reactors, and flow configurations. When activity unit is inverse minutes, the time can be overestimated due to the lack of information on PGM mass mentioned in footnote ^a. ^fApplied potential could not be determined with respect to the standard hydrogen electrode (SHE) because the electrolyte concentration was not provided for the reference electrode used.

Electrocatalytic continuous flow reactor designs include plate-in-tank reactors,^{93–98} packed,^{96,99,100} moving,⁹⁶ or fluidized bed reactors,^{96,97,101} flow-through membrane reactors,²⁶ and parallel-plate thin layer flow reactors (Figure 2d–g).^{100,102–107} Comparisons of reaction rates and reaction times are again provided in Table 3. The shortest reaction time for NO₂⁻ (1.2 min) was obtained from a recent parallel-plate thin layer reactor study; those for NO₃⁻ are in a similar range except for one study (0.03 min) performed in a single compartment batch cell with a high over potential (−1.25 V/SCE). In all cases, reduction occurs at the cathode, while oxidation (typically of water) occurs at the anode. The cathode and anode are often in different chambers separated by a proton exchange membrane; this avoids reoxidation of reduced nitrogen species back to NO₃⁻ at the anode.²⁷ In some cases, a reference electrode is used to control the applied potential;^{26,95} otherwise the reactor is operated in galvanostatic mode at a constant current.^{102–107} An advantage of controlling the potential is the ability to control hydrogen evolution.²⁷ The standard potential for atomic hydrogen generation is higher than that for molecular hydrogen generation, so atomic hydrogen can be used as the electron donor if the potential required for NO₃⁻ reduction is below that for atomic hydrogen but over that for molecular hydrogen. As addressed in more detail later, this can maximize hydrogen use and provide control for N₂ instead of NH₄⁺.

The plate-in-tank reactor is the most studied electrocatalytic reactor in the laboratory^{93–96,98} and is used in industry for water electrolysis, etc.¹²⁰ It consists of an open tank with solid plates or rod electrodes, typically with water in the upflow direction. In some cases, inert millimeter-sized particles are placed between the electrodes and fluidized to improve mixing.^{96,97,101} In addition to plate-in-tank reactors, electrocatalytically active particles or spheres are alternatively used as electrodes in packed bed and moving bed reactors to increase the electroactive surface area for reaction.^{96,99,100} In comparison to a common plate-in-tank reactor, the moving bed reactor (but not the packed bed reactor) showed improved activity and current efficiency.⁹⁶ This was attributed to increased mass transfer caused by intensive mixing from the moving bed and continuous surface renewal of the cathode particles from mechanical friction. The unfavorable performance of the packed bed reactor was attributed to poor charge circulation and uneven current distribution across the catalytically active particles. The moving bed reactor can also suffer from the adverse effect of uneven current distribution on reduction activity, especially with high applied current.^{27,96}

Several electrocatalytic membrane reactors have been proposed in the literature,²⁶ with encouraging results such as fast kinetics due to a flow-through configuration and a fair-to-good current efficiency. Among the most promising, is one where Pd with either In or Cu was loaded onto a three-dimensional magnéli phase TiO₂ membrane and used for NO₃⁻ reduction.²⁶ Reaction rate constants were relatively high (0.016 L g_{metal}⁻¹ min⁻¹), and a model fitted to the experiments at different flow rates indicates mass transfer is not limiting. Also, the current efficiency was high, despite the large overpotential required for reduction. This is due to the low flow rate through the reactor that allowed balanced nitrate and hydrogen consumption. While promising, further work is needed to improve reactor design to reduce cell potential, lower energy consumption, and to demonstrate scale up of

both materials and flow rates with fast NO_3^- reduction kinetics and high current efficiency.

Thin-layer reactors^{102,104–107} also show promise for minimizing mass transfer limitations and approaching reaction rates measured in batch systems. This technology is widely used in chloro-alkali industry and involves creating thin sheets of fluid flowing over the cathode and/or anode.¹²⁰ The thin sheet configuration allows a reference electrode to be positioned near the working electrode for potential control and minimizes the mass transfer length scale to the electrode surface. Such a design was proposed in our recent work,⁴⁹ and NO_2^- reduction rates approaching those in batch reactors ($0.38 \text{ L g}_{\text{Pd}}^{-1} \text{ min}^{-1}$) were obtained with only generation of atomic hydrogen at an applied potential of -0.6 V vs Ag/AgCl at pH 6.5. A reactive transport model demonstrated that overall reaction rates were primarily limited by reaction kinetics and that improvements in catalyst activity could result in twice the amount of nitrite removal in 2 h. While promising, this design still needs to be evaluated for nitrate reduction. However, the use of similar reactors in the chloro-alkali industry indicates that scale-up is promising.

■ EFFORTS TO REDUCE PLATINUM GROUP METAL USE THROUGH MATERIAL DESIGN

Improvements in intrinsic reaction rates can boost overall treatment rates and reduce catalyst needs when mass transfer is not limiting. Efforts to achieve such improvements are primarily focused on advanced material design. As illustrated in Figure 3(a–c), most nitrate reduction catalysts consist of a

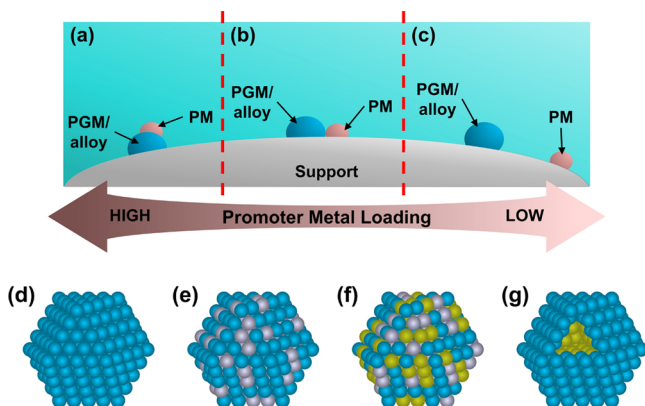


Figure 3. (a–c) Relative locations of PGM or PGM alloy and PM. In general, more promoter metal nanoparticles are located closer to PGM/alloys with increased loading of the former. (d) Platinum group metal nanoparticles with (e) one or (f) two alloyed non-PGMs and a (g) core–shell configuration.

platinum-group metal (usually Pd) and a promoter metal (Cu, In, or Sn) dispersed on a common support (*i.e.*, silica, alumina, or activated carbon). Metal types and loadings have been varied to improve performance. In most cases, platinum (Pt) and Pd combined with either Cu or In have resulted in the fastest reduction rates in catalytic systems and have been primarily used in electrocatalytic systems. PGM loadings vary but are typically between 0.1 to 5.0 wt %, with optimal values from 0.1 to 1%.^{11,30,63,121} PM loadings also vary, though it is generally agreed that the optimal PGM:PM ratio ranges from 4:1 to 10:1.^{29,30,63,70,89,122} Lower PGM:PM ratios generally correspond to increasing coverage of PGM surfaces with PM.

To reduce costs, a number of efforts have evaluated substituting in part or whole nonplatinum-group or less expensive metals for Pd or Pt. As illustrated in Figure 3e–g, partial substitution involves creating core@shell structures or alloys, either of which decreases PGM requirements. Most core@shell combinations combine a gold (Au) core with a decorated Pd or Pt outlayer. Nitrite reduction rate enhancements with respect to PGM requirements are 8.2–14.4 times that of monometallic PdNPs. However, Au is similar in price to PGMs ($\$57.19 \text{ g}_{\text{Au}}^{-1}$ vs $\$63.77 \text{ g}_{\text{Pd}}^{-1}$; APMEC, Inc., as of 6/29/2020), and nitrite reduction rate enhancements relative to total precious metals are more modest, 1.3–2.3 times.^{72,123} Alloy structures involve substituting non-PGMs into the PGM lattice. The first attempt at this for NO_2^- reduction substituted Cu for Pd. Maximum NO_2^- reduction rate enhancements (~ 32.7 times) were observed with the unsupported $\text{Pd}_{80}\text{Cu}_{20}\text{NPs}$ ($1.67 \text{ vs } 0.044 \text{ L g}_{\text{metal}}^{-1} \text{ min}^{-1}$).²³ More recently, Au and silver (Ag) have separately been substituted into the Pd lattice; NO_2^- rate enhancements of 2.56-times and 2.31-times were observed with $\sim 50\%$ substitution of Au ($5.12 \text{ vs } 2.0 \text{ L g}_{\text{metal}}^{-1} \text{ min}^{-1}$) and $\sim 10\%$ substitution of Ag ($4.38 \text{ vs } 1.35 \text{ L g}_{\text{metal}}^{-1} \text{ min}^{-1}$), respectively,^{24,115} and these maximum rates are higher than those reported for the Cu–Pd alloy NPs. While encouraging, it is not yet clear if these rate enhancements correspond to NO_3^- reduction rates, where hydrogen spillover is required.

In catalyst studies, complete replacement of PGM has been achieved in only a limited number of cases. The typical metals used are nickel (Ni) or iron (Fe). Ni-based catalysts rely on secondary metals (*e.g.*, zirconium¹²⁴) to replenish the reduced catalyst metal or aqueous species to help reduce NO_3^- (*e.g.*, hydrazine monohydrate, N_2H_4).¹²⁵ Fe-based catalysts show some activity at circumneutral pH but require much lower pH ranges (~ 3.3) for efficient reduction of NO_3^- .¹²⁶ Recently, a Ni_2P catalyst showed promise for NO_3^- hydrogenation. However, the catalyst also requires a low pH (*i.e.*, ≤ 4) for reaction; at pH 7, the catalyst converted less than 25% of the original NO_3^- concentration after 24 h.¹²⁷ Another drawback that many non-PGM catalysts face is poor selectivity ($\leq 10\%$) to N_2 . While NH_4^+ production and recovery is promising in industrial wastes where NO_3^- (and post-treatment, NH_4^+) levels are high, the costs of concentrating the final NH_4^+ is prohibitively high for the relatively low levels seen in drinking water treatment.

In electrochemical studies, NO_3^- reduction has been evaluated without the use of precious metals. Cu,^{94,101,128–130} Ni,¹²⁸ Fe,^{27,99} Sn,^{101,111} Bi,¹²⁹ and Co_3O_4 ⁶¹ have all been shown to be active for electrochemical NO_3^- reduction, of which Cu seems to have the best activity. However, Cu is highly selective for NH_4^+ as the end product, which is not ideal for drinking water treatment.^{27,94,101,128,130} Other metals such as Ni,^{27,94} Fe,⁹⁹ and Bi¹²⁹ showed mixed selectivity, while P-doped Co_3O_4 and Sn cathode exhibited high N_2 selectivity. The overpotentials required for NO_3^- reduction using these metal cathodes are relatively high compared to those using PGMs, and generally exceed the H_2 evolution potential. Therefore, most studies reported poor current efficiency due to the waste of electrons to H_2 evolution.^{61,101,111,128} High overpotential also leads to high energy consumption. Another major problem associated with these nonprecious metal cathodes is stability. Corrosion of cathode and leaching of metal ions into the treated water hinders the performance of the electrochemical process and

poses significant environmental concern and health risk even though some metals such as Sn or Bi are not regulated by the U.S. EPA.^{27,94,99,111}

Other efforts to increase intrinsic reaction rates have focused on modifying catalyst supports, often with the goal of increasing catalyst dispersion or modifying the electronic configuration of active metals to enhance nitrate reduction rates. Catalyst dispersion is measured using TEM or carbon monoxide adsorption, and higher support surface areas often correspond to greater catalyst dispersion and activity per mass of precious metal. Catalyst electronic configuration or state is a less well-defined concept, and no generally recognized parameters are used for assessment. As a result, researchers have evaluated NO_3^- and NO_2^- reduction rates on supports with greater electronic conductivity (e.g., carbon nanotubes, carbon nanofibers, graphene), and on supports that are more easily reduced or oxidized. No general trend for NO_3^- or NO_2^- reduction has emerged, but this may be due to the lack of systematic comparisons of similar supports with small differences in a single property.

More clear insights regarding electronic properties have been gained from studies that evaluated hydrogen spillover on carefully prepared surfaces. Precision-enhanced top-down synthetic methods have allowed researchers to fabricate tunable model systems to study the extent of hydrogen spillover on certain metal oxides. In 2017, Karim et al. used electron beam lithography to construct 16 distinct systems: one lone iron oxide island and 15 pairs of iron oxide–platinum nanoparticles where the distance between the iron oxide and platinum islands were methodically increased from overlapping (i.e., 0 nm) to 45 nm.⁵⁷ These systems were placed on either an aluminum oxide (alumina) support or a titanium oxide (titania) support (i.e., nonreducible vs reducible, respectively) to evaluate the effect on hydrogen spillover. The platinum particles adsorbed and dissociated molecular hydrogen, and atomic hydrogen that spilled over reduced the iron oxide. The researchers used X-ray photoemission electron microscopy (X-PEEM) to monitor the oxidation state of the iron and therefore the extent of activated hydrogen spillover. When the alumina support was used, pairs separated by more than 15 nm displayed no iron reduction, and even at 5 nm there was little iron reduction. However, when the titania support was used, all systems (including the lone iron oxide particle with no nearby platinum) displayed maximum reduction of iron regardless of separation distance. X-ray adsorption spectroscopy (XAS) revealed that the titanium in the support was reduced by hydrogen, which only occurred with platinum present. Translating such trends to nitrate reduction is less clear, however, because the influence of the promoter metal and nitrate adsorption is unknown.^{131,132}

■ CHALLENGES FOR CATALYST LONGEVITY

Improvements to catalyst longevity also reduce PGM costs by increasing replacement intervals. Catalyst longevity is decreased by foulants, which adsorb and block catalyst sites. Examples are natural organic matter (NOM), biological growth, and reduced sulfur species such as sulfide (S^{2-}). NOM may be less of a concern, because its adsorption was easily reversed by washing with an alkaline solution (pH 11) for several hours.¹³³ There is evidence that unwanted biological growth reduced nitrate reduction activities in a long-term trickle-bed-reactor study,³⁴ indicating periodic treatment with a strong oxidant or acid is likely required for

prevention. Sulfide, by contrast, is a known catalyst poison and more concerning. Only a handful of studies have evaluated its removal. Only one aqueous phase oxidant, hypochlorite (ClO^-), was shown to be effective.^{118,134} Treatment with it resulted in recovery of 39% the original NO_3^- reduction activity on a Pd/In catalyst.¹¹⁸ However, sufficient buffer was required to prevent a drop in pH to 4.2 and rapid Pd (but not In) leaching. Regeneration with ClO^- , or the presence of 1000 mg/L Cl^- , also promoted Cu leaching from Pd/Cu catalysts,²² indicating In is the preferred promoter metal when acidic and/or saline conditions are anticipated. Not effective at regeneration of the Pd/In catalyst were two other aqueous phase oxidants, hydrogen peroxide and oxygenated water, and most effective was oxidizing the catalyst in heated air.¹¹⁸ With the latter approach, 60% of the original NO_3^- reduction activity was recovered. Any potential advantages of using electrocatalysis to facilitate regeneration have yet to be explored. It seems reasonable that this could be performed by reversing electrode polarity and oxidizing foulants, but metal leaching concerns must be evaluated.

Catalysts have also been shown to lose activity over repeated use in the absence of any obvious foulants. In many studies, catalyst activity decreases when subject to repeated batch cycles of nitrate or nitrite treatment, e.g., by 35 to 45% over five to ten cycles.^{24,115} However, some studies show little to no loss in activity over repeated cycles.^{23,63} In two recent studies, a Pd–In on activated carbon catalyst was used to treat NO_3^- continuously over 3 weeks of operation in a trickle bed reactor fed a countercurrent feed of gas phase hydrogen.¹⁰ Here, the activity only dropped 15% over 21 days. It is possible that a larger drop in activity occurred in the first few hours or days, but the measurement resolution did not allow capture of such a trend. Hence, in the absence of foulants, initial drops in activity in batch studies appear to stabilize when catalysts are operated in the continuous mode for many days and weeks.

■ CHALLENGES FOR SAFE AND EFFICIENT USE OF ATOMIC HYDROGEN AND END-PRODUCT SELECTIVITY

Transporting and storing molecular hydrogen represents a safety concern, and widespread implementation of a catalytic nitrate reduction technology likely requires generating this chemical on-site as needed,²⁵ or eliminating generation of molecular hydrogen altogether and only using atomic hydrogen. Commercial on-site generators are available for molecular hydrogen generation, and this can be mixed into the treatment stream. However, this approach still requires hydrogen gas handling, and atomic hydrogen generation within a reactor using a built-in cathode seems more promising for long-term sustainability. An alternative solution is to use formic acid. This nonflammable solute donates hydrogen and yields CO_2 at PGM surfaces, providing both an electron donor and buffer.^{29,70} Both higher and lower nitrate reduction rates have been observed with formic acid versus hydrogen,²⁹ and this appears to be function of the ratio of PGM to PM sites. Formic acid appears to favor lower ratios, as transfer hydrogenation from this chemical to nitrate is proposed to occur only at interfaces between the PGM and PM; molecular hydrogen (by contrast) appears to favor higher ratios because atomic hydrogen spillover from PGM to PM surfaces allows NO_3^- reduction on isolated PM surfaces. Most NO_3^- reduction studies have used molecular hydrogen as the electron donor, and additional studies showing the strengths

and weaknesses of formic acid as the hydrogen source are needed.

Efficient use of hydrogen is coupled to safe use of hydrogen. Ideally, only atomic hydrogen is generated, or molecular hydrogen is consumed within the retention time of a reactor so that it does not have to be captured as off-gas and/or recycled back to the front of the reactor.⁸³ This requires matching hydrogen generation rates to nitrate consumption rates within a reactor, or matching the current applied for atomic hydrogen generation with nitrate consumption rates within a reactor.

End-product selectivity of NO_3^- reduction for either N_2 or NH_4^+ is ultimately controlled by the ratio of hydrogen to nitrogen species on PGM surfaces.^{25,29,70,78,135–138} At lower ratios, nitrogen pairing is favored and more N_2 is formed. At higher ratios, nitrogen hydrogenation is favored, and more NH_4^+ is formed. Therefore, end-product selectivity can be controlled by managing molecular hydrogen to NO_3^- ratios at the inlet of catalytic reactors,^{33,70,136} and by controlling atomic or molecular hydrogen production rates within electrocatalytic reactors.¹³⁹ In the latter case, Yan et al. showed that the production of molecular hydrogen can be eliminated when nitrite reduction is promoted above -0.61 vs Ag/AgCl reference electrode in a pH 6.5 electrolyte.⁴⁹ This approach favors complete hydrogen utilization because no off-gassing occurs, and it favors N_2 production by limiting hydrogen coverage on the catalyst surface.

End-product selectivity can also be controlled by solution pH^{25,29,71,78} and by the choice of catalyst materials.^{30,31,76,84,138,140} At elevated pH, adsorption of anionic nitrogen species decreases, and this favors greater hydrogen to nitrogen ratios.²⁵ As a result, the reaction favors NH_4^+ production. Different materials have different affinities for nitrogen species and atomic hydrogen, and this affects end-product selectivity. For example, under similar conditions, use of Pd favors N_2 production, while use of Pt, Ir, Rh, and Ru favors NH_4^+ production.^{30,138,140,141} In a recent study evaluating NO_2^- reduction,¹⁴¹ relative H coverage was evaluated by DFT calculation of stepwise adsorption energies of H onto Ir(111) and Pd(111) surfaces. Maximum H coverage is estimated when the adsorption energy reaches zero, which is ~ 1.3 for Ir(111) and 1.0 for Pd(111). This shows that Ir(111) can thermodynamically accommodate more H on the surface than Pd(111). The resulting higher H:N ratio therefore leads to greater ammonium selectivity on Ir versus Pd. This finding was further generalized to H coverage on transition metals: larger orbitals of 5d transition metals compared to 4d transition metals leads to stronger interactions with H and correspondingly higher theoretical H surface coverages under ambient conditions; hence, the higher H coverage promotes NH_4^+ as the end product. Therefore, Pd based catalysts with relatively low H coverage have been most widely studied for catalytic nitrate reduction due to its better selectivity toward N_2 .

Prioritization of Technology Challenges and Implications for Achieving Regulatory Acceptance

The primary challenges to address for widespread adoption of (electro)catalytic treatment for nitrate removal in water treatment plants are PGM costs, efficient and safe hydrogen usage, and end-product selectivity for N_2 . The most challenging of these is reducing PGM costs. Still needed is a scalable reactor with negligible mass transfer limitations to

reduce PGM requirements. Several promising reactor configurations have been proposed in the literature, and the most promising are those based on electrocatalytic reduction that couple hydrogen production at PGM surfaces with high electrode-water interfacial areas. The former eliminates H_2 gas-to-water mass transfer limitations, and the latter minimizes boundary layer mass transfer limitations. However, all electrochemical reactors presented thus far in the literature require large overpotentials to treat NO_3^- , and this corresponds to wasted energy and material wear. Therefore, a key priority for research is developing a scalable electrocatalytic reactor that can treat NO_3^- with an applied potential above that corresponding to H_2 evolution.

Although PGM requirements for existing NO_3^- reduction catalysts appear competitive with IX (Table 2), further improvements in catalyst activity have the potential to make (electro)catalytic NO_3^- reduction a more attractive option. Alloy catalysts show promise for many hydrogenation reactions at the PGM surface, but their ability to enhance NO_3^- reduction that occurs via hydrogen spillover on a promoter metal surface has yet to be demonstrated. Also promising are nonprecious metal catalysts. However, those developed to date require either low pH operating conditions and/or produce almost exclusively NH_4^+ . While the latter is a valuable product, its removal from water comes with additional expenses and risk that has not been sufficiently evaluated. Hence, another key priority for research is catalysts with greater activity per unit of precious metal, or better yet catalysts that select for N_2 with no precious metals.

Catalyst longevity is another factor that significantly impacts PGM costs. NO_3^- reduction activities for a variety of catalyst formulations have been shown to continually decrease over repeated cycles of treatment in batch reactors. However, longer-term continuous treatment studies in flow-through reactors suggest this decrease is transient and catalyst activity approaches a plateau assuming known foulants are not present. The presence of foulants presents another challenge, with NOM, biological growth, and reduced sulfur species being the most problematic identified thus far. Fortunately, NOM fouling appears to be easily reversed, and biomass growth can likely be prevented with periodic cleaning. However, sulfur species may require removal before catalytic treatment, and the best approach is not yet clear. Hence, another key area of research is to identify sustainable strategies to electrocatalytically treat NO_3^- in sulfur-containing waters.

Efficient and safe hydrogen use is the next highest priority. While no less important than decreasing PGM costs, the technical ability to address this concern using formic acid, or with *in situ* electrochemical or electrocatalytic production has been realized. The challenge is integrating this know-how into the handful of most successful reactors under evaluation at scale. A related priority is selecting for the end product N_2 . With careful control of hydrogen feed or production, end-product selectivity for N_2 is enhanced. Another approach to control for N_2 selectivity is catalyst selection; Pd appears to be the metal of choice, either alone or combined with another metal. Another key priority for research is to identify nonprecious metal catalysts formulations that select for N_2 .

Fortunately, IX is a reliable and readily available technology for nitrate removal from drinking water. Unfortunately, its use comes at considerable environmental and financial cost. Water treatment professionals recognize these limitations and are open to alternatives. Catalytic and electrocatalytic treatment

offer attractive alternatives, but uncertainty associated primarily with platinum group metal use presents too large a barrier for most water treatment professionals to invest in pilot scale studies of this technology. Such studies are critically needed to more accurately address this unknown, build confidence in the technology, and promote regulatory acceptance and eventual large-scale implementation.

AUTHOR INFORMATION

Corresponding Author

Charles J. Werth — Department of Civil, Architectural, and Environmental Engineering, The University of Texas at Austin, Austin, Texas 78712, United States;  orcid.org/0000-0002-8492-5523; Email: werth@utexas.edu

Authors

Chenxu Yan — Department of Civil, Architectural, and Environmental Engineering, The University of Texas at Austin, Austin, Texas 78712, United States;  orcid.org/0000-0002-2227-5510

Jacob P. Troutman — Department of Civil, Architectural, and Environmental Engineering, The University of Texas at Austin, Austin, Texas 78712, United States; Department of Chemistry, The University of Austin at Texas, Austin, Texas 78712, United States;  orcid.org/0000-0002-2026-8886

Complete contact information is available at:

<https://pubs.acs.org/10.1021/acsestengg.0c00076>

Notes

The authors declare no competing financial interest.

ACKNOWLEDGMENTS

Funding for this work was provided by the National Science Foundation under Grant Nos. CBET-1706797 (C.Y.), CBET-1922504 (C.J.W.), and DGE-1828974 (J.P.T.).

REFERENCES

- (1) Spalding, R. F.; Exner, M. E. Occurrence of Nitrate in Groundwater—A Review. *J. Environ. Qual.* **1993**, *22* (3), 392–402.
- (2) Dubrovsky, N. M.; Burow, K. R.; Clark, G. M.; Gronberg, J. A. M.; Hamilton, P. A.; Hitt, K. J.; Mueller, D. K.; Munn, M. D.; Nolan, B. T.; Puckett, L. J.; Rupert, M. G.; Short, T. M.; Spahr, N. E.; Sprague, L. A.; Wilber, W. G. *The Quality of Our Nation's Waters—Nutrients in the Nation's Streams and Groundwater, 1992–2004: U.S. Geological Survey Circular 1350*; U.S. Geological Survey, 2010.
- (3) National Primary Drinking Water Regulations; EPA 816-F-09-004; U.S. Environmental Protection Agency, 2009.
- (4) Brockway, D. G.; Urie, D. H. Determining Sludge Fertilization Rates for Forests from Nitrate-N in Leachate and Groundwater. *J. Environ. Qual.* **1983**, *12* (4), 487–492.
- (5) Tindall, J. A.; Lull, K. J.; Gaggiani, N. G. Effects of Land Disposal of Municipal Sewage Sludge on Fate of Nitrates in Soil, Streambed Sediment, and Water Quality. *J. Hydrol.* **1994**, *163* (1–2), 147–185.
- (6) Avery, A. A. Infantile Methemoglobinemia: Reexamining the Role of Drinking Water Nitrates. *Environ. Health Perspect.* **1999**, *107* (7), 583–586.
- (7) Wolff, I. A.; Wasserman, A. E. Nitrates, Nitrites, and Nitrosamines. *Science* **1972**, *177* (4043), 15–19.
- (8) Wang, L.; Chen, A. S. C.; Tong, N.; Coonfare, C. T. *Arsenic Removal from Drinking Water by Ion Exchange U.S. EPA Demonstration Project at Fruitland, ID—Six-Month Evaluation Report*; Washington, D.C., 2007.
- (9) Wang, L.; Chen, A. S. C.; Wang, A.; Condit, W. E. *Arsenic and Nitrate Removal from Drinking Water by Ion Exchange U.S. EPA Demonstration Project at Vale, OR—Final Performance Evaluation Report*; 2011.
- (10) Bergquist, A. M.; Choe, J. K.; Strathmann, T. J.; Werth, C. J. Evaluation of a Hybrid Ion Exchange-Catalyst Treatment Technology for Nitrate Removal from Drinking Water. *Water Res.* **2016**, *96*, 177–187.
- (11) Choe, J. K.; Bergquist, A. M.; Jeong, S.; Guest, J. S.; Werth, C. J.; Strathmann, T. J. Performance and Life Cycle Environmental Benefits of Recycling Spent Ion Exchange Brines by Catalytic Treatment of Nitrate. *Water Res.* **2015**, *80*, 267–280.
- (12) Jensen, V. B.; Darby, J. L. Brine Disposal Options for Small Systems in California's Central Valley. *Journal of the American Water Works Association* **2016**, *108* (5), E276–E289.
- (13) Vitousek, P. M.; Aber, J. D.; Howarth, R. W.; Likens, G. E.; Matson, P. A.; Schindler, D. W.; Schlesinger, W. H.; Tilman, D. G. Human Alteration of the Global Nitrogen Cycle: Sources and Consequences. *Ecological Applications* **1997**, *7* (3), 737–750.
- (14) Galloway, J. N.; Townsend, A. R.; Erisman, J. W.; Bekunda, M.; Cai, Z.; Freney, J. R.; Martinelli, L. A.; Seitzinger, S. P.; Sutton, M. A. Transformation of the Nitrogen Cycle: Recent Trends, Questions, and Potential Solutions. *Science* **2008**, *320* (5878), 889–892.
- (15) Cañedo-Argüelles, M.; Kefford, B. J.; Piscart, C.; Prat, N.; Schäfer, R. B.; Schulz, C.-J. Salinisation of Rivers: An Urgent Ecological Issue. *Environ. Pollut.* **2013**, *173*, 157–167.
- (16) Kapoor, A.; Viraraghavan, T. Nitrate Removal From Drinking Water—Review. *J. Environ. Eng.* **1997**, *123* (4), 371–380.
- (17) Painter, H. A. A Review of Literature on Inorganic Nitrogen Metabolism in Microorganisms. *Water Res.* **1970**, *4* (6), 393–450.
- (18) Matějů, V.; Čižinská, S.; Krejčí, J.; Janoch, T. Biological Water Denitrification—A Review. *Enzyme Microb. Technol.* **1992**, *14* (3), 170–183.
- (19) Akunna, J. C.; Bizeau, C.; Moletta, R. Nitrate Reduction by Anaerobic Sludge Using Glucose at Various Nitrate Concentrations: Ammonification, Denitrification and Methanogenic Activities. *Environ. Technol.* **1994**, *15* (1), 41–49.
- (20) Amant, P. P. St.; McCarty, P. L. Treatment of High Nitrate Waters. *J. - Am. Water Works Assoc.* **1969**, *61* (12), 659–662.
- (21) Bouwer, E. J.; Crowe, P. B. Biological Processes in Drinking Water Treatment. *J. - Am. Water Works Assoc.* **1988**, *80* (9), 82–93.
- (22) Chaplin, B. P.; Roundy, E.; Guy, K. A.; Shapley, J. R.; Werth, C. J. Effects of Natural Water Ions and Humic Acid on Catalytic Nitrate Reduction Kinetics Using an Alumina Supported Pd–Cu Catalyst. *Environ. Sci. Technol.* **2006**, *40* (9), 3075–3081.
- (23) Guy, K. A.; Xu, H.; Yang, J. C.; Werth, C. J.; Shapley, J. R. Catalytic Nitrate and Nitrite Reduction with Pd–Cu/PVP Colloids in Water: Composition, Structure, and Reactivity Correlations. *J. Phys. Chem. C* **2009**, *113*, 8177–8185.
- (24) Seraj, S.; Kunal, P.; Li, H.; Henkelman, G.; Humphrey, S. M.; Werth, C. J. PdAu Alloy Nanoparticle Catalysts: Effective Candidates for Nitrite Reduction in Water. *ACS Catal.* **2017**, *7* (5), 3268–3276.
- (25) Chaplin, B. P.; Reinhard, M.; Schneider, W. F.; Schüth, C.; Shapley, J. R.; Strathmann, T. J.; Werth, C. J. Critical Review of Pd-Based Catalytic Treatment of Priority Contaminants in Water. *Environ. Sci. Technol.* **2012**, *46* (7), 3655–3670.
- (26) Gayen, P.; Spataro, J.; Avasarala, S.; Ali, A. M.; Cerrato, J. M.; Chaplin, B. P. Electrocatalytic Reduction of Nitrate Using Magnéli Phase TiO₂ Reactive Electrochemical Membranes Doped with Pd-Based Catalysts. *Environ. Sci. Technol.* **2018**, *52* (16), 9370–9379.
- (27) Garcia-Segura, S.; Lanzarini-Lopes, M.; Hristovski, K.; Westerhoff, P. Electrocatalytic Reduction of Nitrate: Fundamentals to Full-Scale Water Treatment Applications. *Appl. Catal., B* **2018**, *236*, 546–568.
- (28) Vorlop, K.; Tacke, T. Erste Schritte Auf Dem Weg Zur Edelmetall-Katalysierten Nitrat- Und Nitrit-Entfernung Aus Trinkwasser. *Chem. Ing. Tech.* **1989**, *61* (10), 836–837.
- (29) Prusse, U.; Vorlop, K. D. Supported Bimetallic Palladium Catalysts for Water-Phase Nitrate Reduction. *J. Mol. Catal. A: Chem.* **2001**, *173* (1–2), 313–328.

(30) Hörold, S.; Vorlop, K. D.; Tacke, T.; Sell, M. Development of Catalysts for a Selective Nitrate and Nitrite Removal from Drinking Water. *Catal. Today* **1993**, *17*, 21–30.

(31) Martínez, J.; Ortiz, A.; Ortiz, I. State-of-the-Art and Perspectives of the Catalytic and Electrocatalytic Reduction of Aqueous Nitrates. *Appl. Catal., B* **2017**, *207*, 42–59.

(32) Pintar, A.; Batista, J. Catalytic Hydrogenation of Aqueous Nitrate Solutions in Fixed-Bed Reactors. *Catal. Today* **1999**, *53* (1), 35–50.

(33) Bergquist, A. M.; Bertoche, M.; Gildert, G.; Strathmann, T. J.; Werth, C. J. Catalytic Denitrification in a Trickle Bed Reactor: Ion Exchange Waste Brine Treatment. *Journal of the American Water Works Association* **2017**, *109* (5), E129–E143.

(34) Bertoche, M.; Bergquist, A. M.; Gildert, G.; Strathmann, T. J.; Werth, C. J. Catalytic Nitrate Removal in a Trickle Bed Reactor: Direct Drinking Water Treatment. *Journal of the American Water Works Association* **2017**, *109* (5), E144–E157.

(35) Meyer, K. J.; Swaim, P. D.; Bellamy, W. D.; Rittmann, B. E.; Tang, Y.; Scott, R.; CH2M HILL. *Biological and Ion Exchange Nitrate Removal Evaluation*; 2010.

(36) Clifford, D.; Lin, C.-C.; Horng, L.-L.; Boegel, J. *Nitrate Removal from Drinking Water in Glendale, Arizona*; 1987.

(37) Jensen, V. B.; Darby, J. L.; Seidel, C.; Gorman, C. *Drinking Water Treatment for Nitrate*; Center for Watershed Sciences, University of California, Davis: Davis, CA, 2012.

(38) California Water Plant Treats Nitrates and Perchlorate with No Liquid Waste. <https://www.kuritaamerica.com/the-splash/california-water-plant-treats-nitrates-and-perchlorate-with-no-liquid-waste> (accessed May 15, 2020).

(39) Guter, G. A. Nitrate Removal from Contaminated Groundwater by Anion Exchange. In *Ion Exchange Technology: Advances in Pollution Control*; Sengupta, A. K., Ed.; CRC Press, 1995.

(40) California Water Services Company Treats Nitrate and Perchlorate in Community Water System. <https://www.evoqua.com/en/brands/IPS/Pages/CA-Water-Service-CO-CS.aspx> (accessed May 15, 2020).

(41) *Nitrate Removal Facility Fact Sheet*; Des Moines Water Works 2015.

(42) Elmer, M. Water Works plans \$15 million for expanded nitrate facility <https://www.desmoinesregister.com/story/news/2017/05/25/water-works-plans-%0A15-million-expanded-nitrate-facility/336648001/> (accessed May 15, 2020).

(43) Vedachalam, S.; Mandelia, A. J.; Heath, E. The impact of source water quality on the cost of nitrate treatment. *AWWA Wat. Sci.* **2019**, *1*, e1011.

(44) Naidenko, O. V.; Cox, C.; Bruzelius, N. *TROUBED WATERS Farm Pollution Threatens Drinking Water*; 2012.

(45) FAQ's about Nitrate in Columbus' Drinking Water. <https://www.columbus.gov/NitrateFAQs/> (accessed May 15, 2020).

(46) Nitrate Contamination—What Is the Cost? Minnesota Department of Agriculture and Department of Health, 2004.

(47) Swanson, S. Continuous Ion Exchange Technology Utilized to Combat Rising Nitrate Levels <https://www.kuritaamerica.com/the-splash/continuous-ion-exchange-%0Atechnology-utilized-to-combat-rising-nitrate-levels> (accessed May 15, 2020).

(48) Choe, J. K.; Mehnert, M. H.; Guest, J. S.; Strathmann, T. J.; Werth, C. J. Comparative Assessment of the Environmental Sustainability of Existing and Emerging Perchlorate Treatment Technologies for Drinking Water. *Environ. Sci. Technol.* **2013**, *47* (9), 4644–4652.

(49) Yan, C.; Kakuturu, S.; Butzlaaff, A.; Cwiertny, D. M.; Mubeen, S.; Werth, C. J. Scalable Reactor Design for Electrocatalytic Nitrite Reduction with Minimal Mass Transfer Limitations. *ACS ES&T Eng.* **2020**, in review.

(50) Nikolaidis, P.; Poullikkas, A. A Comparative Overview of Hydrogen Production Processes. *Renewable Sustainable Energy Rev.* **2017**, *67*, 597–611.

(51) Austin Energy. Austin Energy Rates—Cents per kilowatt hour by customer class <https://data.austintexas.gov/Utilities-and-City-Services/Austin-Energy-Rates-Cents-per-kilowatt-hour-by-cus/scy3-ke5d> (accessed Jul 1, 2020).

(52) Jung, J.; Bae, S.; Lee, W. Nitrate Reduction by Maghemite Supported Cu-Pd Bimetallic Catalyst. *Appl. Catal., B* **2012**, *127*, 148–158.

(53) Hamid, S.; Kumar, M. A.; Lee, W. Highly Reactive and Selective Sn-Pd Bimetallic Catalyst Supported by Nanocrystalline ZSM-5 for Aqueous Nitrate Reduction. *Appl. Catal., B* **2016**, *187*, 37–46.

(54) Guo, S.; Heck, K.; Kasiraju, S.; Qian, H.; Zhao, Z.; Grabow, L. C.; Miller, T.; Wong, M. S. Insights into Nitrate Reduction over Indium-Decorated Palladium Nanoparticle Catalysts. *ACS Catal.* **2018**, *8*, 503–515.

(55) Spreafico, C.; Karim, W.; Ekinci, Y.; van Bokhoven, J. A.; VandeVondele, J. Hydrogen Adsorption on Nanosized Platinum and Dynamics of Spillover onto Alumina and Titania. *J. Phys. Chem. C* **2017**, *121*, 17862–17872.

(56) Prins, R.; Palfi, V. K.; Reiher, M. Hydrogen Spillover to Nonreducible Supports. *J. Phys. Chem. C* **2012**, *116* (27), 14274–14283.

(57) Karim, W.; Spreafico, C.; Kleibert, A.; Gobrecht, J.; VandeVondele, J.; Ekinci, Y.; van Bokhoven, J. A. Catalyst Support Effects on Hydrogen Spillover. *Nature* **2017**, *541* (7635), 68–71.

(58) Adams, B. D.; Chen, A. The Role of Palladium in a Hydrogen Economy. *Mater. Today* **2011**, *14* (6), 282–289.

(59) Cabria, I.; López, M. J.; Fraile, S.; Alonso, J. A. Adsorption and Dissociation of Molecular Hydrogen on Palladium Clusters Supported on Graphene. *J. Phys. Chem. C* **2012**, *116* (40), 21179–21189.

(60) Granja, A.; Alonso, J. A.; Cabria, I.; López, M. J. Competition between Molecular and Dissociative Adsorption of Hydrogen on Palladium Clusters Deposited on Defective Graphene. *RSC Adv.* **2015**, *5* (59), 47945–47953.

(61) Gao, J.; Jiang, B.; Ni, C.; Qi, Y.; Bi, X. Enhanced Reduction of Nitrate by Noble Metal-Free Electrocatalysis on P-Doped Three-Dimensional Co₃O₄ Cathode: Mechanism Exploration from Both Experimental and DFT Studies. *Chem. Eng. J.* **2020**, *382*, 123034.

(62) Mao, R.; Huang, C.; Zhao, X.; Ma, M.; Qu, J. Dechlorination of Tricosan by Enhanced Atomic Hydrogen-Mediated Electrochemical Reduction: Kinetics, Mechanism, and Toxicity Assessment. *Appl. Catal., B* **2019**, *241*, 120–129.

(63) Marchesini, F. A.; Irusta, S.; Querini, C.; Miró, E. Spectroscopic and Catalytic Characterization of Pd-In and Pt-In Supported on Al₂O₃ and SiO₂, Active Catalysts for Nitrate Hydrogenation. *Appl. Catal., A* **2008**, *348* (1), 60–70.

(64) Ebbesen, S. D.; Mojet, B. L.; Lefferts, L. In Situ ATR-IR Study of Nitrite Hydrogenation over Pd/Al₂O₃. *J. Catal.* **2008**, *256* (1), 15–23.

(65) Sá, J.; Anderson, J. A. FTIR Study of Aqueous Nitrate Reduction over Pd/TiO₂. *Appl. Catal., B* **2008**, *77* (3–4), 409–417.

(66) Wärn, J.; Turunen, I.; Salmi, T.; Maunula, T. Kinetics of Nitrate Reduction in Monolith Reactor. *Chem. Eng. Sci.* **1994**, *49* (24), 5763–5773.

(67) Zhang, R.; Shuai, D.; Guy, K. A.; Shapley, J. R.; Strathmann, T. J.; Werth, C. J. Elucidation of Nitrate Reduction Mechanisms on a Pd-In Bimetallic Catalyst Using Isotope Labeled Nitrogen Species. *ChemCatChem* **2013**, *5* (1), 313–321.

(68) Miller, D. D.; Chuang, S. S. C. Pulse Transient Responses of NO Decomposition and Reduction with H₂ on Ag-Pd/Al₂O₃. *J. Phys. Chem. C* **2009**, *113* (33), 14963–14971.

(69) Ebbesen, S. D.; Mojet, B. L.; Lefferts, L. Mechanistic Investigation of the Heterogeneous Hydrogenation of Nitrite over Pt/Al₂O₃ by Attenuated Total Reflection Infrared Spectroscopy. *J. Phys. Chem. C* **2009**, *113* (6), 2503–2511.

(70) Prüss, U.; Hähnlein, M.; Daum, J.; Vorlop, K. D. Improving the Catalytic Nitrate Reduction. *Catal. Today* **2000**, *55* (1–2), 79–90.

(71) Strukul, G.; Gavagnin, R.; Pinna, F.; Modaferrri, E.; Perathoner, S.; Centi, G.; Marella, M.; Tomaselli, M. Use of Palladium Based

Catalysts in the Hydrogenation of Nitrates in Drinking Water: From Powders to Membranes. *Catal. Today* **2000**, *55* (1–2), 139–149.

(72) Li, H.; Guo, S.; Shin, K.; Wong, M. S.; Henkelman, G. Design of a Pd-Au Nitrite Reduction Catalyst by Identifying and Optimizing Active Ensembles. *ACS Catal.* **2019**, *9* (9), 7957–7966.

(73) Pintar, A.; Batista, J.; Levec, J.; Kajiuchi, T. Kinetics of the Catalytic Liquid-Phase Hydrogenation of Aqueous Nitrate Solutions. *Appl. Catal., B* **1996**, *11* (1), 81–98.

(74) Daum, J.; Vorlop, K. D. Kinetic Investigation of the Catalytic Nitrate Reduction: Construction of the Test Reactor System. *Chem. Eng. Technol.* **1999**, *22* (3), 199–202.

(75) Pintar, A.; Batista, J.; Levec, J. Potential of Mono- and Bimetallic Catalysts for Liquid-Phase Hydrogenation of Aqueous Nitrite Solutions. *Water Sci. Technol.* **1998**, *37*, 177–185.

(76) Shuai, D.; Choe, J. K.; Shapley, J. R.; Werth, C. J. Enhanced Activity and Selectivity of Carbon Nanofiber Supported Pd Catalysts for Nitrite Reduction. *Environ. Sci. Technol.* **2012**, *46* (5), 2847–2855.

(77) Daub, K.; Emig, G.; Chollier, M. J.; Callant, M.; Dittmeyer, R. Studies on the Use of Catalytic Membranes for Reduction of Nitrate in Drinking Water. *Chem. Eng. Sci.* **1999**, *54* (10), 1577–1582.

(78) Hörold, S.; Tacke, T.; Vorlop, K. D. Catalytical Removal of Nitrate and Nitrite from Drinking Water: 1. Screening for Hydrogenation Catalysts and Influence of Reaction Conditions on Activity and Selectivity. *Environ. Technol.* **1993**, *14* (10), 931–939.

(79) Matatov-Meytal, U.; Sheintuch, M. Activated Carbon Cloth-Supported Pd-Cu Catalyst: Application for Continuous Water Denitrification. *Catal. Today* **2005**, *102*–103, 121–127.

(80) Aristizábal, A.; Contreras, S.; Divins, N. J.; Llorca, J.; Medina, F. Effect of Impregnation Protocol in the Metallic Sites of Pt-Ag/Activated Carbon Catalysts for Water Denitrification. *Appl. Surf. Sci.* **2014**, *298*, 75–89.

(81) Pintar, A.; Batista, J.; Levec, J. Catalytic Denitrification: Direct and Indirect Removal of Nitrates from Potable Water. *Catal. Today* **2001**, *66*, 503–510.

(82) Pintar, A.; Batista, J. Catalytic Stepwise Nitrate Hydrogenation in Batch-Recycle Fixed-Bed Reactors. *J. Hazard. Mater.* **2007**, *149* (2), 387–398.

(83) Chaplin, B. P.; Shapley, J. R.; Werth, C. J. The Selectivity and Sustainability of a Pd-In/γ-Al₂O₃ Catalyst in a Packed-Bed Reactor: The Effect of Solution Composition. *Catal. Lett.* **2009**, *130* (1–2), 56–62.

(84) Yoshinaga, Y.; Akita, T.; Mikami, I.; Okuhara, T. Hydrogenation of Nitrate in Water to Nitrogen over Pd – Cu Supported on Active Carbon. *J. Catal.* **2002**, *207*, 37–45.

(85) Calvo, L.; Gilarranz, M. A.; Casas, J. A.; Mohedano, A. F.; Rodriguez, J. J. Denitrification of Water with Activated Carbon-Supported Metallic Catalysts. *Ind. Eng. Chem. Res.* **2010**, *49* (12), 5603–5609.

(86) Mendow, G.; Marchesini, F. A.; Miro, E. E.; Querini, C. A. Evaluation of Pd-in Supported Catalysts for Water Nitrate Abatement in a Fixed-Bed Continuous Reactor. *Ind. Eng. Chem. Res.* **2011**, *50* (4), 1911–1920.

(87) Theologides, C. P.; Savva, P. G.; Costa, C. N. Catalytic Removal of Nitrates from Waters in a Continuous Flow Process: The Remarkable Effect of Liquid Flow Rate and Gas Feed Composition. *Appl. Catal., B* **2011**, *102* (1–2), 54–61.

(88) Marchesini, F. A.; Mendow, G.; Picard, N. P.; Zoppas, F. M.; Aghemo, V. S.; Gutierrez, L. B.; Querini, C. A.; Miró, E. E. PdIn Catalysts in a Continuous Fixed Bed Reactor for the Nitrate Removal from Groundwater. *Int. J. Chem. React. Eng.* **2019**, DOI: 10.1515/ijcre-2018-0126.

(89) Hähnlein, M.; Prüsse, U.; Daum, J.; Morawsky, V.; Kröger, M.; Schröder, M.; Schnabel, M.; Vorlop, K. D. Preparation of Microscopic Catalysts and Colloids for Catalytic Nitrate and Nitrite Reduction and Their Use in a Hollow Fibre Dialyser Loop Reactor. *Stud. Surf. Sci. Catal.* **1998**, *118*, 99–107.

(90) Zhao, Z.; Tong, G.; Tan, X. Nitrite Removal from Water by Catalytic Hydrogenation in a Pd-CNTs/Al₂O₃ Hollow Fiber Membrane Reactor. *J. Chem. Technol. Biotechnol.* **2016**, *91* (8), 2298–2304.

(91) Lüdtke, K.; Peinemann, K. V.; Kasche, V.; Behling, R. D. Nitrate Removal of Drinking Water by Means of Catalytically Active Membranes. *J. Membr. Sci.* **1998**, *151* (1), 3–11.

(92) Wehbe, N.; Guilhaume, N.; Fiaty, K.; Miachon, S.; Dalmon, J. A. Hydrogenation of Nitrates in Water Using Mesoporous Membranes Operated in a Flow-through Catalytic Contactor. *Catal. Today* **2010**, *156* (3–4), 208–215.

(93) Paidar, M.; Rousar, I.; Bouzek, K. Electrochemical Removal of Nitrate Ions in Waste Solutions after Regeneration of Ion Exchange Columns. *J. Appl. Electrochem.* **1999**, *29* (5), 611–617.

(94) Reyter, D.; Bélanger, D.; Roué, L. Optimization of the Cathode Material for Nitrate Removal by a Paired Electrolysis Process. *J. Hazard. Mater.* **2011**, *192* (2), 507–513.

(95) Ding, J.; Li, W.; Zhao, Q. L.; Wang, K.; Zheng, Z.; Gao, Y. Z. Electroreduction of Nitrate in Water: Role of Cathode and Cell Configuration. *Chem. Eng. J.* **2015**, *271*, 252–259.

(96) Paidar, M.; Bouzek, K.; Bergmann, H. Influence of Cell Construction on the Electrochemical Reduction of Nitrate. *Chem. Eng. J.* **2002**, *85* (2–3), 99–109.

(97) Paidar, M.; Bouzek, K.; Jelínek, L.; Matějka, Z. A Combination of Ion Exchange and Electrochemical Reduction for Nitrate Removal from Drinking Water Part II: Electrochemical Treatment of a Spent Regenerant Solution. *Water Environ. Res.* **2004**, *76* (7), 2691–2698.

(98) Szpyrkowicz, L.; Daniele, S.; Radaelli, M.; Specchia, S. Removal of NO₃⁻ from Water by Electrochemical Reduction in Different Reactor Configurations. *Appl. Catal., B* **2006**, *66* (1–2), 40–50.

(99) Kim, H. K.; Jeong, J. Y.; Cho, H. N.; Park, J. Y. Kinetics of Nitrate Reduction with the Packed Bed Iron Bipolar Electrode. *Sep. Purif. Technol.* **2015**, *152*, 140–147.

(100) Bockris, J. O. M.; Kim, J. Electrochemical Treatment of Low-Level Nuclear Wastes. *J. Appl. Electrochem.* **1997**, *27* (6), 623–634.

(101) Máčová, Z.; Bouzek, K.; Šerák, J. Electrocatalytic Activity of Copper Alloys for NO₃⁻ Reduction in a Weakly Alkaline Solution: Part 2: Copper-Tin. *J. Appl. Electrochem.* **2007**, *37* (5), 557–566.

(102) Hasnat, M. A.; Ishibashi, I.; Sato, K.; Agui, R.; Yamaguchi, T.; Ikeue, K.; Machida, M. Electrocatalytic Reduction of Nitrate Using Cu-Pd and Cu-Pt Cathodes/H⁺-Conducting Solid Polymer Electrolyte Membrane Assemblies. *Bull. Chem. Soc. Jpn.* **2008**, *81* (12), 1675–1680.

(103) Machida, M.; Sato, K.; Ishibashi, I.; Hasnat, M. A.; Ikeue, K. Electrocatalytic Nitrate Hydrogenation over an H⁺-Conducting Solid Polymer Electrolyte Membrane-Modified Cathode Assembly. *Chem. Commun.* **2006**, No. 7, 732–734.

(104) Hasnat, M. A.; Ben Aoun, S.; Rahman, M. M.; Asiri, A. M.; Mohamed, N. Lean Cu-Immobilized Pt and Pd Films/H⁺-Conducting Membrane Assemblies: Relative Electrocatalytic Nitrate Reduction Activities. *J. Ind. Eng. Chem.* **2015**, *28*, 131–137.

(105) Cheng, H.; Scott, K.; Christensen, P. A. Application of a Solid Polymer Electrolyte Reactor to Remove Nitrate Ions from Wastewater. *J. Appl. Electrochem.* **2005**, *35* (6), 551–560.

(106) Jha, K.; Weidner, J. W. Evaluation of Porous Cathodes for the Electrochemical Reduction of Nitrates and Nitrites in Alkaline Waste Streams. *J. Appl. Electrochem.* **1999**, *29* (11), 1305–1315.

(107) Genders, J. D.; Hartsough, D.; Hobbs, D. T. Electrochemical Reduction of Nitrates and Nitrites in Alkaline Nuclear Waste Solutions. *J. Appl. Electrochem.* **1996**, *26* (1), 1–9.

(108) Hasnat, M. A.; Agui, R.; Hinokuma, S.; Yamaguchi, T.; Machida, M. Different Reaction Routes in Electrocatalytic Nitrate/Nitrite Reduction Using an H⁺-Conducting Solid Polymer Electrolyte. *Catal. Commun.* **2009**, *10* (7), 1132–1135.

(109) Hasnat, M. A.; Karim, M. R.; Machida, M. Electrocatalytic Ammonia Synthesis: Role of Cathode Materials and Reactor Configuration. *Catal. Commun.* **2009**, *10* (15), 1975–1979.

(110) Brylev, O.; Sarrazin, M.; Roué, L.; Bélanger, D. Nitrate and Nitrite Electrocatalytic Reduction on Rh-Modified Pyrolytic Graphite Electrodes. *Electrochim. Acta* **2007**, *52* (21), 6237–6247.

(111) Katsounaros, I.; Ipsakis, D.; Polatides, C.; Kyriacou, G. Efficient Electrochemical Reduction of Nitrate to Nitrogen on Tin Cathode at Very High Cathodic Potentials. *Electrochim. Acta* **2006**, *52* (3), 1329–1338.

(112) Wang, Y.; Qu, J.; Wu, R.; Lei, P. The Electrocatalytic Reduction of Nitrate in Water on Pd/Sn-Modified Activated Carbon Fiber Electrode. *Water Res.* **2006**, *40* (6), 1224–1232.

(113) Ghodbane, O.; Sarrazin, M.; Roué, L.; Bélanger, D. Electrochemical Reduction of Nitrate on Pyrolytic Graphite-Supported Cu and Pd–Cu Electrocatalysts. *J. Electrochem. Soc.* **2008**, *155* (6), F117.

(114) Lan, H.; Liu, X.; Liu, H.; Liu, R.; Hu, C.; Qu, J. Efficient Nitrate Reduction in a Fluidized Electrochemical Reactor Promoted by Pd-Sn/AC Particles. *Catal. Lett.* **2016**, *146* (1), 91–99.

(115) Troutman, J. P.; Li, H.; Haddix, A. M.; Kienzle, B. A.; Henkelman, G.; Humphrey, S. M.; Werth, C. J. PdAg Alloy Nanocatalysts: Toward Economically Viable Nitrite Reduction in Drinking Water. *ACS Catal.* **2020**, *10*, 7979–7989.

(116) Lemaignen, L.; Tong, C.; Begon, V.; Burch, R.; Chadwick, D. Catalytic Denitrification of Water with Palladium-Based Catalysts Supported on Activated Carbons. *Catal. Today* **2002**, *75* (1–4), 43–48.

(117) Gavagnin, R.; Biassetto, L.; Pinna, F.; Strukul, G. Nitrate Removal in Drinking Waters: The Effect of Tin Oxides in the Catalytic Hydrogenation of Nitrate by Pd/SnO₂ Catalysts. *Appl. Catal., B* **2002**, *38* (2), 91–99.

(118) Chaplin, B. P.; Shapley, J. R.; Werth, C. J. Regeneration of Sulfur-Fouled Bimetallic Pd-Based Catalysts. *Environ. Sci. Technol.* **2007**, *41* (15), 5491–5497.

(119) Ilinich, O. M.; Cuperus, F. P.; Van Gemert, R. W.; Gribov, E. N.; Nosova, L. V. Catalytic Membrane in Denitrification of Water: A Means to Facilitate Intraporous Diffusion of Reactants. *Sep. Purif. Technol.* **2000**, *21* (1–2), 55–60.

(120) Pletcher, D.; Walsh, F. C. Electrochemical Engineering. In *Industrial Electrochemistry*; Pletcher, D., Walsh, F. C., Eds.; Springer Netherlands: Dordrecht, 1993; pp 60–172.

(121) Yin, Y. B.; Guo, S.; Heck, K. N.; Clark, C. A.; Coonrod, C. L.; Wong, M. S. Treating Water by Degrading Oxyanions Using Metallic Nanostructures. *ACS Sustainable Chem. Eng.* **2018**, *6* (9), 11160–11175.

(122) Marchesini, F. A.; Irusta, S.; Querini, C.; Miro, E. Nitrate Hydrogenation over Pt_xIn/Al₂O₃ and Pt_xIn/SiO₂. Effect of Aqueous Media and Catalyst Surface Properties upon the Catalytic Activity. *Catal. Commun.* **2008**, *9*, 1021–1026.

(123) Qian, H.; Zhao, Z.; Velazquez, J. C.; Pretzer, L. A.; Heck, N.; Wong, M. S. Supporting Palladium Metal on Gold Nanoparticles Improves Its Catalysis for Nitrite Reduction[†]. *Nanoscale* **2014**, *6*, 358–364.

(124) Mikami, I.; Yoshinaga, Y.; Okuhara, T. Rapid Removal of Nitrate in Water by Hydrogenation to Ammonia with Zr-Modified Porous Ni Catalysts. *Appl. Catal., B* **2004**, *49* (3), 173–179.

(125) Rai, R. K.; Tyagi, D.; Singh, S. K. Room-Temperature Catalytic Reduction of Aqueous Nitrate to Ammonia with Ni Nanoparticles Immobilized on an Fe₃O₄@n-SiO₂@h-SiO₂–NH₂ Support. *Eur. J. Inorg. Chem.* **2017**, *2017* (18), 2450–2456.

(126) Shukla, A.; Pande, J. V.; Banswal, A.; Osiceanu, P.; Biniwale, R. B. Catalytic Hydrogenation of Aqueous Phase Nitrate over Fe/C Catalysts. *Catal. Lett.* **2009**, *131* (3–4), 451–457.

(127) Wei, L.; Liu, D.-J.; Rosales, B. A.; Evans, J. W.; Vela, J. Mild and Selective Hydrogenation of Nitrate to Ammonia in the Absence of Noble Metals. *ACS Catal.* **2020**, *10*, 3618–3628.

(128) Bouzek, K.; Paidar, M.; Sadílková, A.; Bergmann, H. Electrochemical Reduction of Nitrate in Weakly Alkaline Solutions. *J. Appl. Electrochem.* **2001**, *31* (11), 1185–1193.

(129) Gao, W.; Gao, L.; Li, D.; Huang, K.; Cui, L.; Meng, J.; Liang, J. Removal of Nitrate from Water by the Electrocatalytic Denitrification on the Cu-Bi Electrode. *J. Electroanal. Chem.* **2018**, *817*, 202–209.

(130) Abdallah, R.; Geneste, F.; Labasque, T.; Djelal, H.; Fourcade, F.; Amrane, A.; Taha, S.; Floner, D. Selective and Quantitative Nitrate Electroreduction to Ammonium Using a Porous Copper Electrode in an Electrochemical Flow Cell. *J. Electroanal. Chem.* **2014**, *727*, 148–153.

(131) Soares, O. S. G. P.; Órfão, J. J. M.; Pereira, M. F. R. Nitrate Reduction in Water Catalysed by Pd – Cu on Different Supports. *Desalination* **2011**, *279* (1–3), 367–374.

(132) Wada, K.; Hirata, T.; Hosokawa, S.; Iwamoto, S.; Inoue, M. Effect of Supports on Pd–Cu Bimetallic Catalysts for Nitrate and Nitrite Reduction in Water. *Catal. Today* **2012**, *185* (1), 81–87.

(133) Knitt, L. E.; Shapley, J. R.; Strathmann, T. J. Rapid Metal-Catalyzed Hydrodehalogenation of Iodinated X-Ray Contrast Media. *Environ. Sci. Technol.* **2008**, *42* (2), 577–583.

(134) Chaplin, B. P.; Shapley, J. R.; Werth, C. J. Oxidative Regeneration of Sulfide-Fouled Catalysts for Water Treatment. *Catal. Lett.* **2009**, *132* (1–2), 174–181.

(135) De Vooy, A. C. A.; Van Santen, R. A.; Van Veen, J. A. R. Electrocatalytic Reduction of NO-3 on Palladium/Copper Electrodes. *J. Mol. Catal. A: Chem.* **2000**, *154* (1–2), 203–215.

(136) Shin, H.; Jung, S.; Bae, S.; Lee, W.; Kim, H. Nitrite Reduction Mechanism on a Pd Surface. *Environ. Sci. Technol.* **2014**, *48* (21), 12768–12774.

(137) Pintar, A.; Šetinc, M.; Levec, J. Hardness and Salt Effects on Catalytic Hydrogenation of Aqueous Nitrate Solutions. *J. Catal.* **1998**, *174* (1), 72–87.

(138) Huo, X.; Van Hoomissen, D. J.; Liu, J.; Vyas, S.; Strathmann, T. J. Hydrogenation of Aqueous Nitrate and Nitrite with Ruthenium Catalysts. *Appl. Catal., B* **2017**, *211*, 188–198.

(139) Hasnat, M. A.; Ahamad, N.; Nizam Uddin, S. M.; Mohamed, N. Silver Modified Platinum Surface/H + Conducting Nafion Membrane for Cathodic Reduction of Nitrate Ions. *Appl. Surf. Sci.* **2012**, *258* (7), 3309–3314.

(140) Soares, O. S. G. P.; Órfão, J. J. M.; Ruiz-Martínez, J.; Silvestre-Albero, J.; Sepúlveda-Escribano, A.; Pereira, M. F. R. Pd–Cu/AC and Pt–Cu/AC Catalysts for Nitrate Reduction with Hydrogen: Influence of Calcination and Reduction Temperatures. *Chem. Eng. J.* **2010**, *165* (1), 78–88.

(141) Li, H.; Yan, C.; Guo, H.; Shin, K.; Humphrey, S. M.; Werth, C. J.; Henkelman, G. Cu_xIr_{1-x} Nanoalloy Catalysts Achieve Near 100% Selectivity for Aqueous Nitrite Reduction to NH₃. *ACS Catal.* **2020**, *10*, 7915.